Istituto Nazionale di Fisica Nucleare

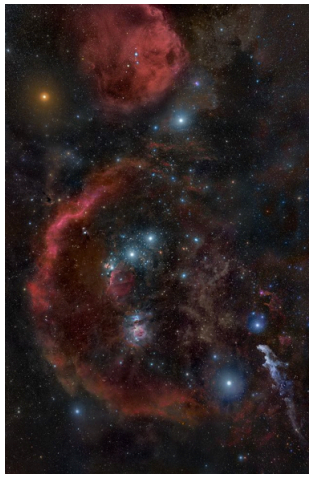

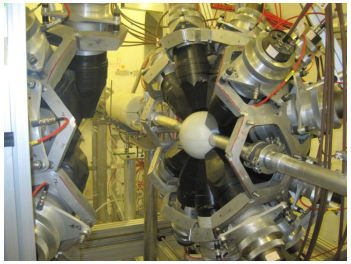

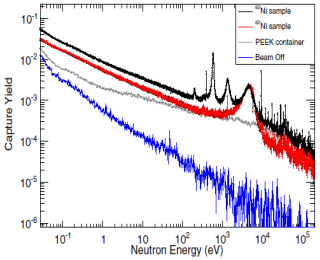

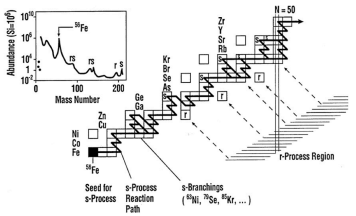

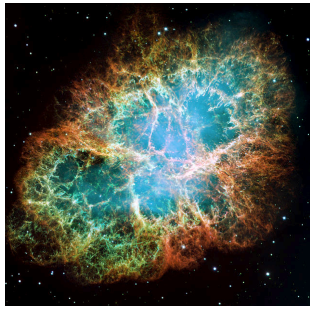

Data for *s process* from **n_TOF**

NIC XV

Nuclear data and Astrophysics

Cristian Massimi

for the n_TOF Collaboration

nTOF

Outline

- **The n_TOF project**

  Objectives, basic parameters, instrumentation

- **Examples of measurements and their impact on *s-process nucleosynthesis***

  Branch-point isotopes, neutron sources, *s-only* isotopes, *s-process* bottleneck, weak component

- **Future program**

  Facility upgrade 2019-2021, measurements 2021-2030

The n_TOF project

1. Atominstitut, Technische Universität Wien, Austria
2. University of Vienna, Faculty of Physics, Austria
3. European Commission JRC, Institute for Reference Materials and Measurements (IRMM)
4. Department of Physics, Faculty of Science, University of Zagreb, Croatia
5. Charles University, Prague, Czech Republic
6. Centre National de la Recherche Scientifique/IN2P3 - IPN, Orsay, France
7. Commissariat à l'Énergie Atomique (CEA) Saclay - Irfu, Gif-sur-Yvette, France
8. Johann-Wolfgang-Goethe Universität, Frankfurt, Germany
9. Karlsruhe Institute of Technology, Campus Nord, Institut für Kernphysik, Karlsruhe, Germany
10. National Technical University of Athens (NTUA), Greece
11. Aristotle University of Thessaloniki, Thessaloniki, Greece
12. Bhabha Atomic Research Centre (BARC), Mumbai, India
13. ENEA Bologna e
14. Dipartimento di Fisica, e Astronomia, Università di Bologna
15. Sezione INFN di Bologna, INFN Bari, Bologna, LNL, Perugia, Trieste, LNS
16. Uniwersytet Łódzki, Lodz, Poland
17. Instituto Tecnológico e Nuclear, Instituto Superior Técnico, Universidade Técnica de Lisboa, Portugal
18. Horia Hulubei National Institute of Physics and Nuclear Engineering – Bucharest, Romania
19. Centro de Investigaciones Energeticas Medioambientales y Tecnológicas (CIEMAT), Madrid, Spain
20. Instituto de Fìsica Corpuscular, CSIC-Universidad de Valencia, Spain
21. Universitat Politecnica de Catalunya, Barcelona, Spain
22. Universidad de Sevilla, Spain
23. Universidade de Santiago de Compostela, Spain
24. Department of Physics and Astronomy - University of Basel, Basel, Switzerland
25. European Organization for Nuclear Research (CERN), Geneva, Switzerland
26. Paul Scherrer Institut, Villigen PSI, Switzerland
27. University of Manchester, Oxford Road, Manchester, UK
28. University of York, Heslington, York, UK

~ 130 researchers

The n_TOF project

Istituto Nazionale di Fisica Nucleare

Objective: to provide Nuclear Data for Science (and Technology)

How the elements are synthesized in the Universe?

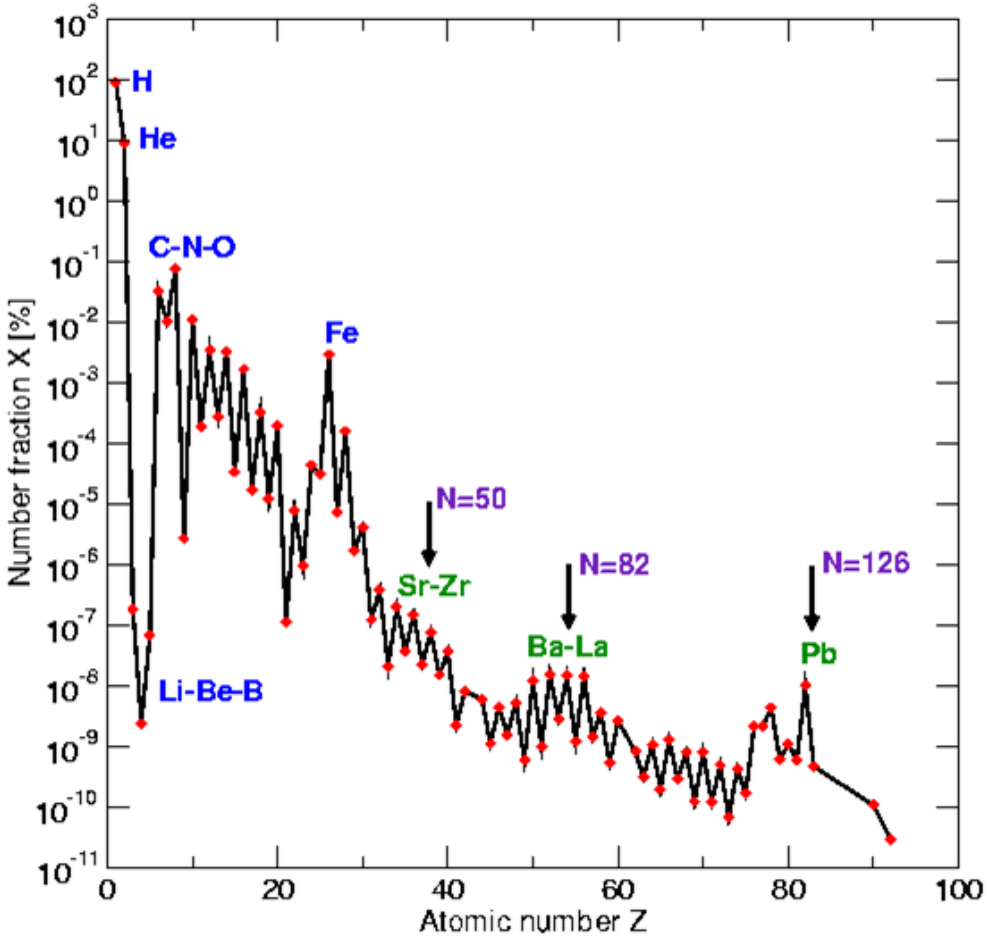

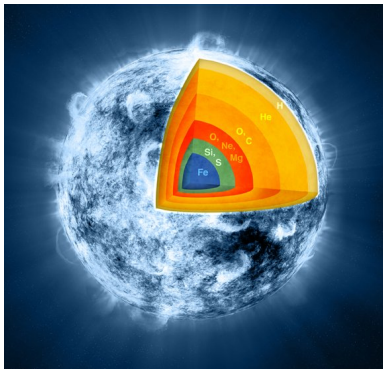

Big Bang

The n_TOF project

Objective: to provide Nuclear Data for Science (and Technology)

How the elements are synthesized in the Universe?

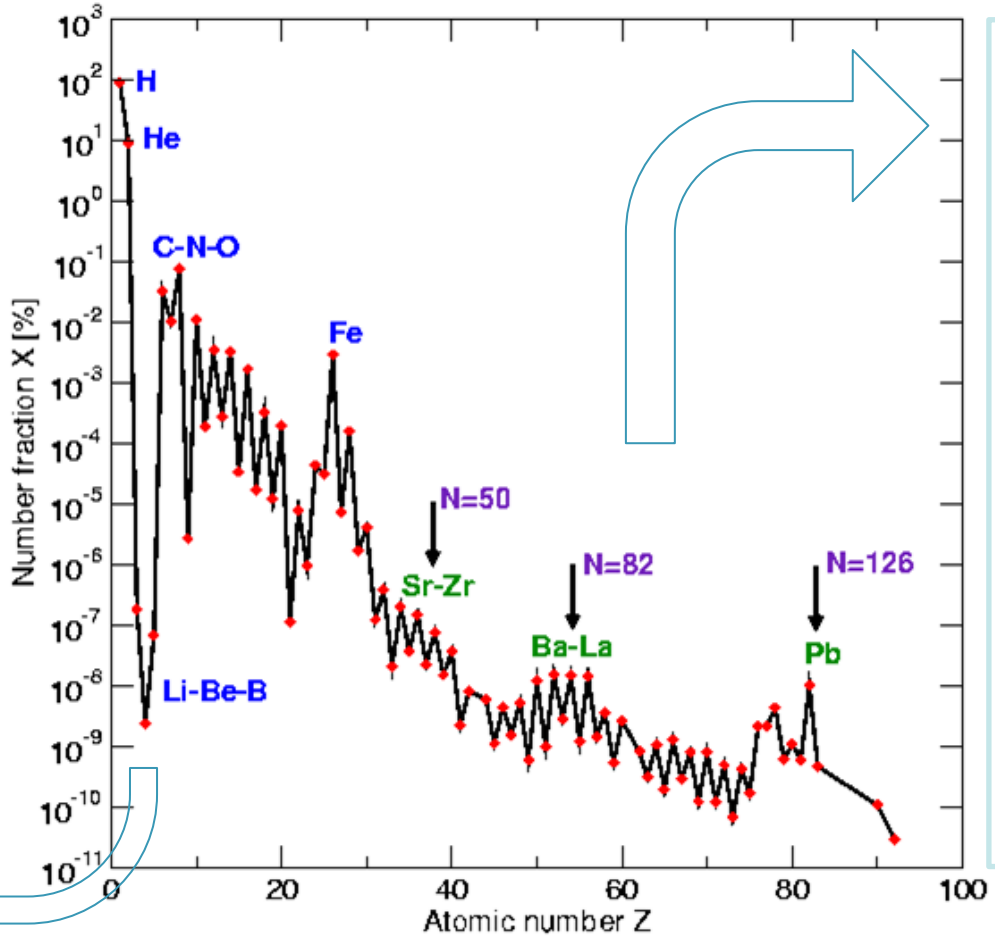

BBN:

- *^{7}Be(n,p) cross section measurement for the Cosmological Lithium Problem at the n_TOF facility at CERN*, L. Damone **Wednesday 27, 10:00**

s process:

- *Neutron induced reactions in Astrophysics*, by C. Lederer, **Wednesday 27 12:00**

Posters

- *The neutron capture cross section measurement of the thallium isotopes ^{203}Tl, ^{204}Tl and ^{205}Tl at the n_TOF facility at CERN*, A. Casanovas
- *Measurement of the ^{16}O(n,α)^{13}C reaction cross-section at the CERN n_TOF facility* – S. Urlass
- *The Stellar ^{72}Ge(n,γ) Cross Section: A First Measurement at n_TOF*, M. Dietz

The n_TOF project

Element production beyond Fe

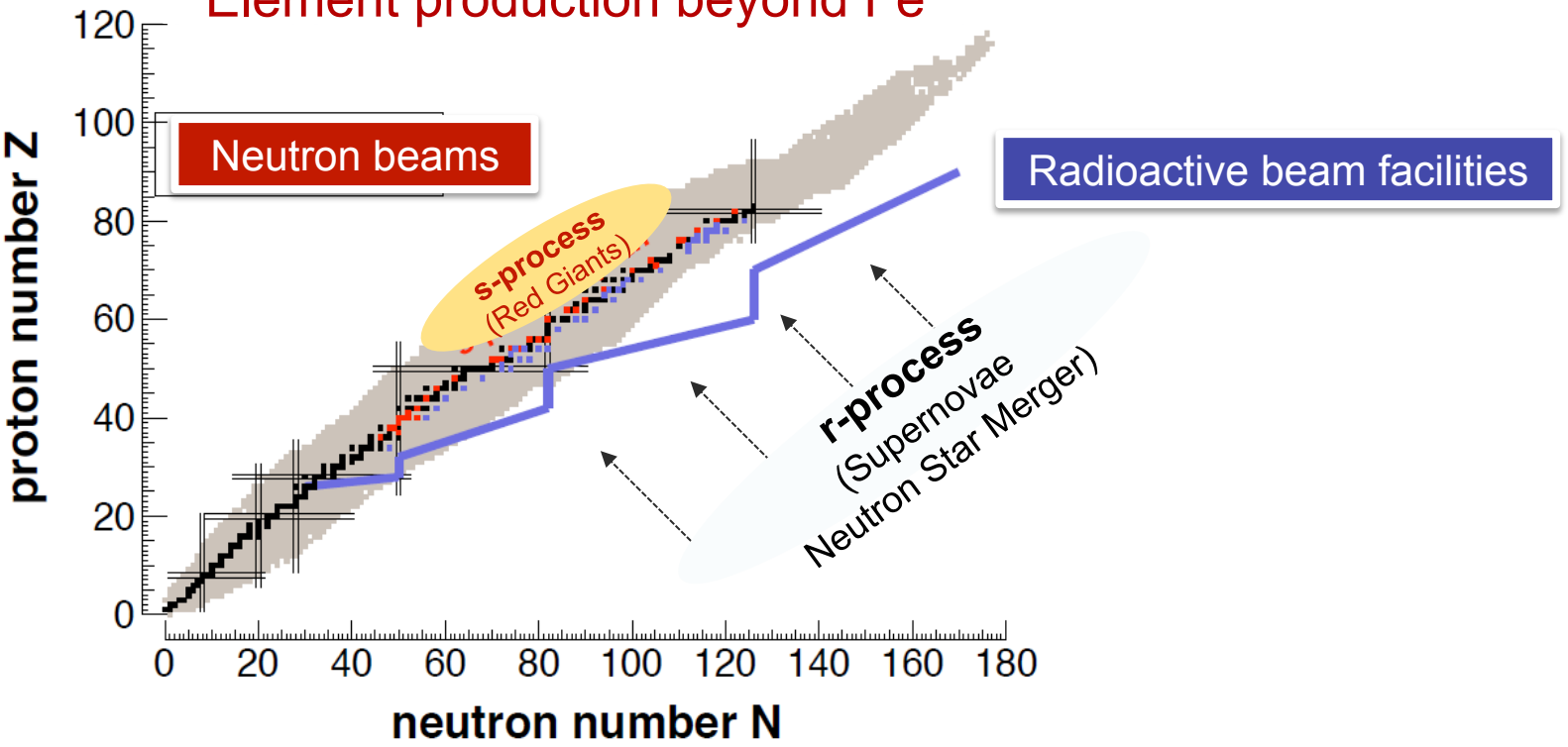

s-process (slow process):

- **Capture times** long relative to decay time
- Involves mostly **stable isotopes**
- $\mathbf{N_n}$ = 10^8 n/cm^3 , $\mathbf{E_n}$ = 0.3 – 300 keV

r-process (rapid process):

- **Capture times** short relative to decay times
- Produces **unstable isotopes** (neutron-rich)
- $\mathbf{N_n}$ = $10^{20\text{-}30}$ n/cm^3

The n_TOF project

s-process nucleosynthesis proceeds through **neutron capture** reactions and successive β **decay.**

The abundance of elements in the Universe depends on:

- **thermodinamic conditions** (temperture and neutron density);
- β-decay rate;
- **neutron capture cross-sections.**

Need of **accurate** (n,γ) cross-sections:

- **refine models** of stellar nucleosynthesis in the Universe;
- obtain information on the **stellar environment and evolution**

key quantity
σ(n,γ)

s process

Along the β-stability valley

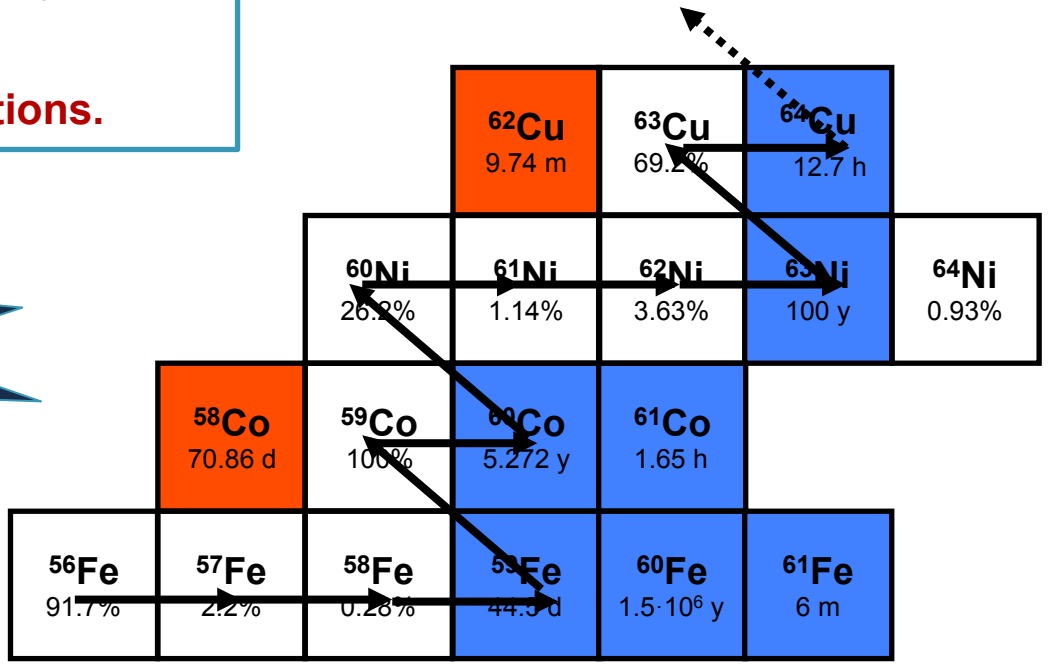

The n_TOF project

Stellar spectra: AGB (8, 23 keV) and Massive stars (25, 90 keV)

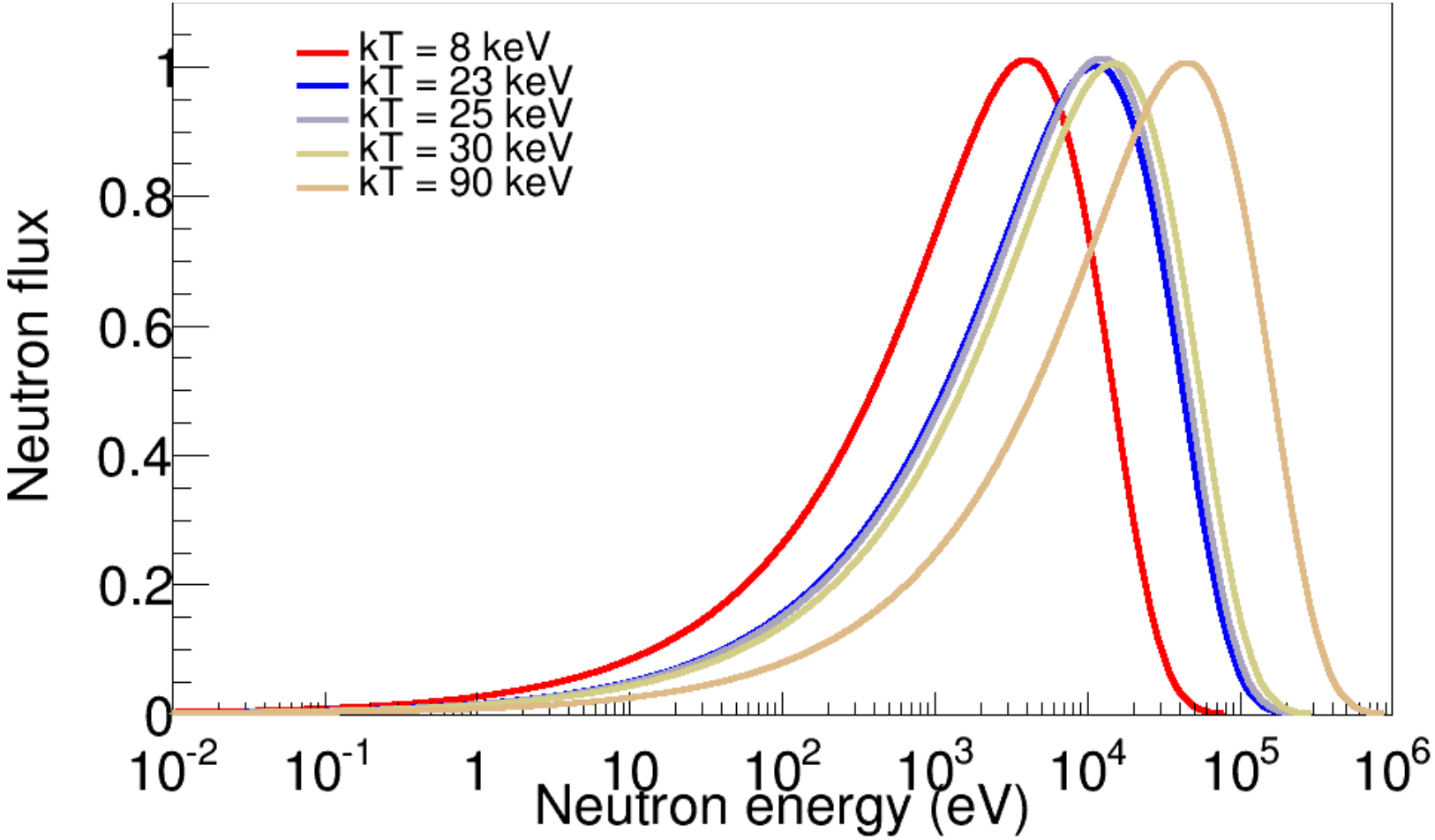

The n_TOF project

Stellar spectra: AGB (8, 23 keV) and Massive stars (25, 90 keV)

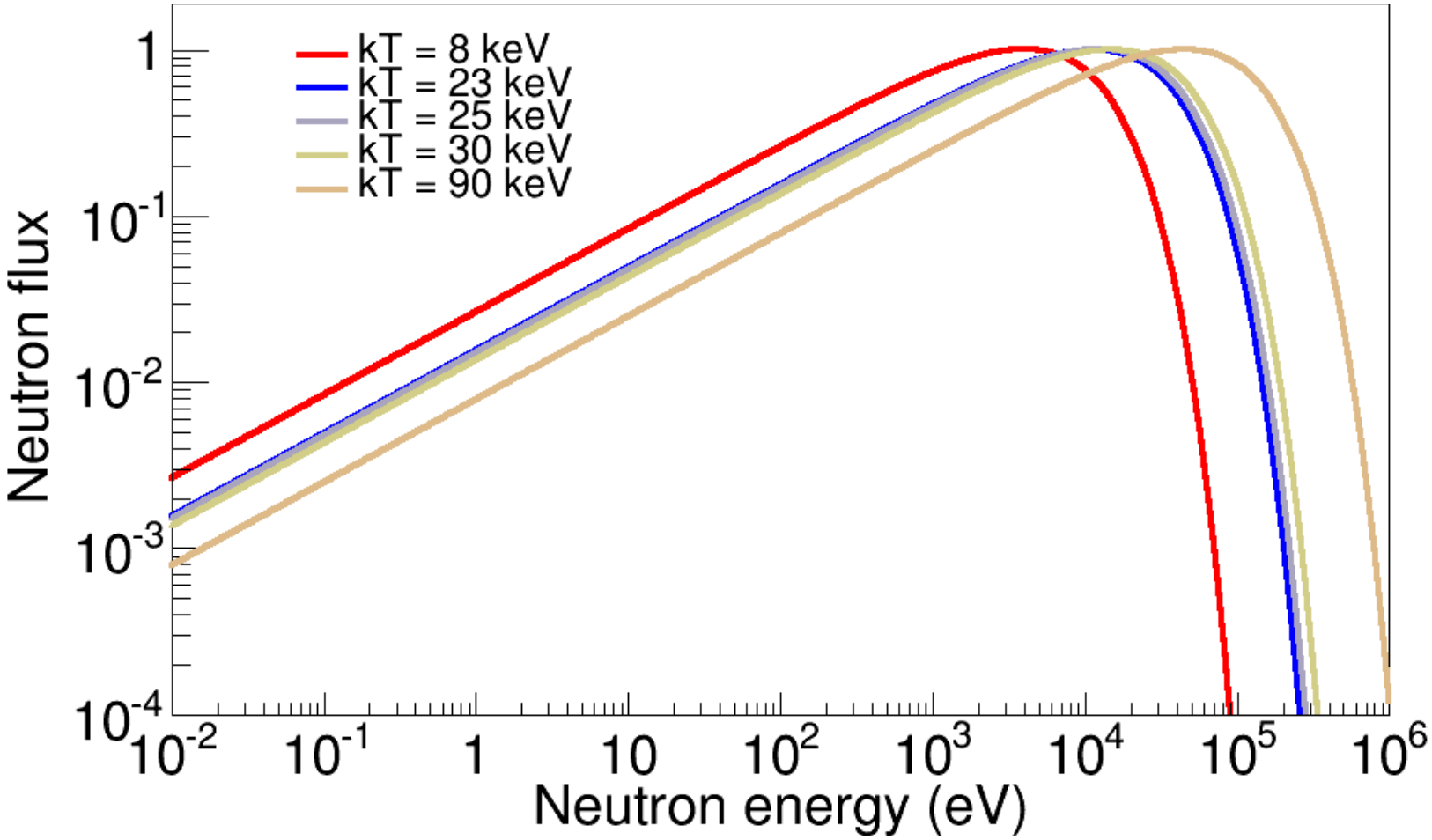

The n_TOF project

Stellar spectra: AGB (8, 23 keV) and Massive stars (25, 90 keV)

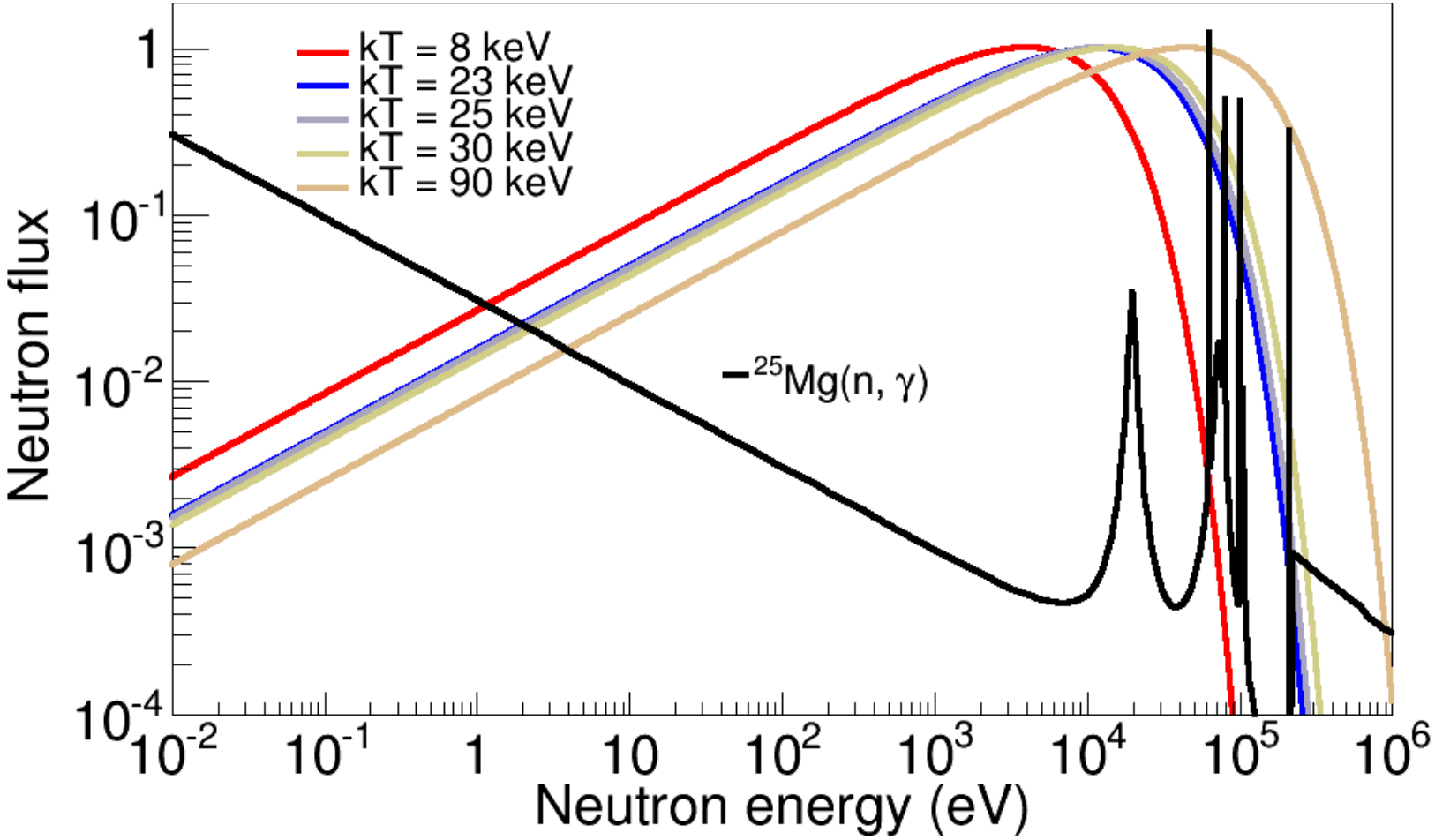

The n_TOF project

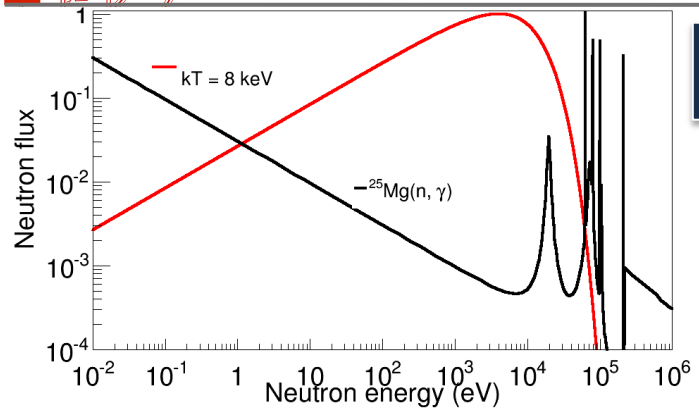

For Astrophysical applications it is important to determine **Maxwellian Averaged Cross-Sections (MACS)**, for various temperatures (kT depends on stellar site).

Reaction rate ($cm^{-3}s^{-1}$): $r = N_A N_n v\sigma(v)$

$$\rightarrow r = N_A N_n \langle \sigma \cdot v \rangle$$

$$MACS \equiv \frac{\langle \sigma \cdot v \rangle}{v_T} = \frac{2}{\sqrt{\pi}(kT)^2} \int_0^\infty \sigma(E) E e^{-E/(kT)} dE$$

The n_TOF project

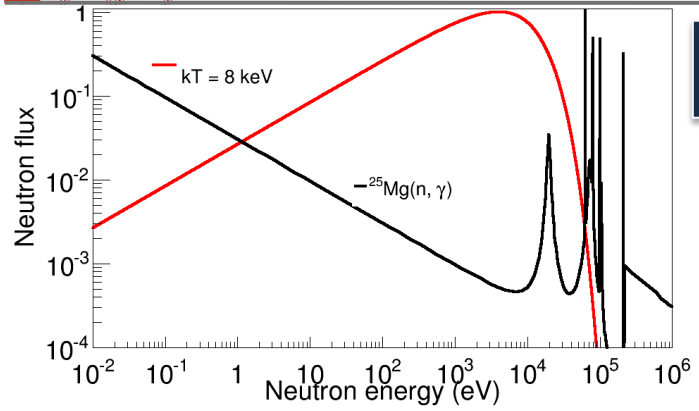

For Astrophysical applications it is important to determine **Maxwellian Averaged Cross-Sections (MACS)**, for various temperatures (kT depends on stellar site).

Reaction rate ($cm^{-3}s^{-1}$): $r = N_A N_n v\sigma(v)$

$$\rightarrow r = N_A N_n \langle \sigma \cdot v \rangle$$

$$MACS \equiv \frac{\langle \sigma \cdot v \rangle}{v_T} = \frac{2}{\sqrt{\pi}(kT)^2} \int_0^\infty \sigma(E) E e^{-E/(kT)} dE$$

Two methods are used to determine MACS:

The n_TOF project

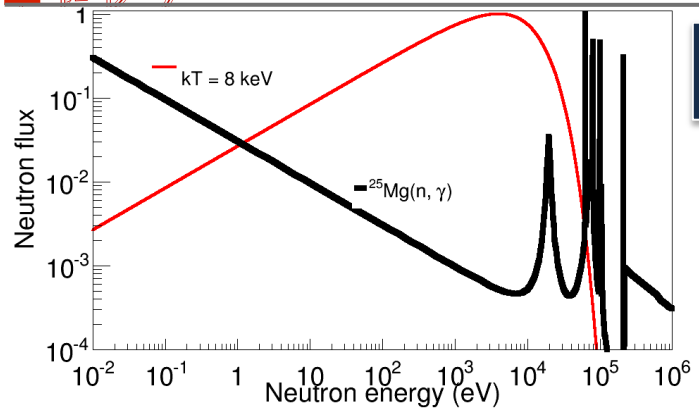

For Astrophysical applications it is important to determine **Maxwellian Averaged Cross-Sections (MACS)**, for various temperatures (kT depends on stellar site).

Reaction rate ($cm^{-3}s^{-1}$): $r = N_A N_n v\sigma(v)$

$$\rightarrow r = N_A N_n \langle \sigma \cdot v \rangle$$

$$MACS \equiv \frac{\langle \sigma \cdot v \rangle}{v_T} = \frac{2}{\sqrt{\pi}(kT)^2} \int_0^\infty \sigma(E) E e^{-E/(kT)} dE$$

Two methods are used to determine MACS:

1. measurement of **energy dependent** neutron capture cross-sections;

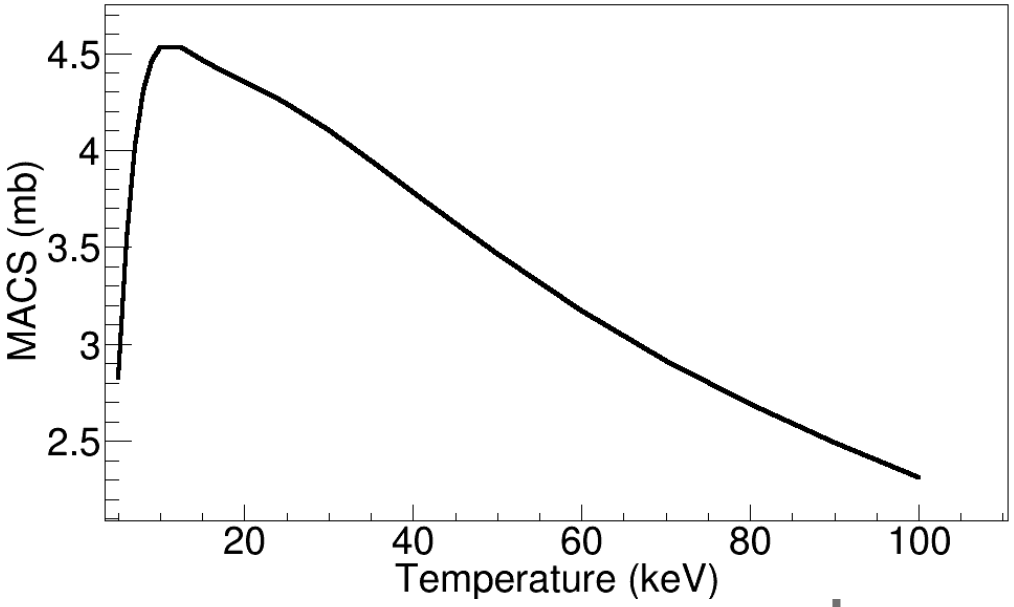

The n_TOF project

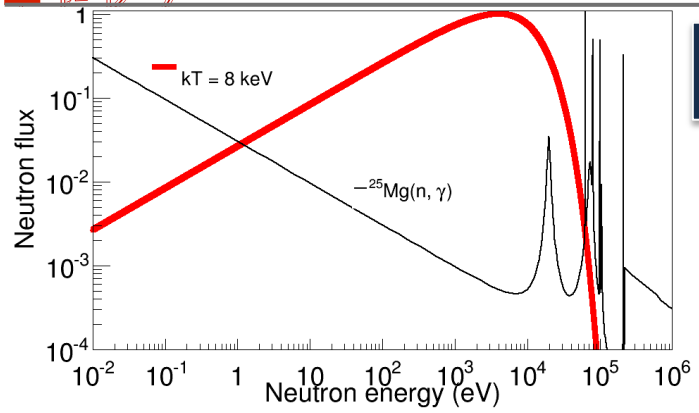

For Astrophysical applications it is important to determine **Maxwellian Averaged Cross-Sections (MACS)**, for various temperatures (kT depends on stellar site).

Reaction rate ($cm^{-3}s^{-1}$): $r = N_A N_n v\sigma(v)$

$$\rightarrow r = N_A N_n \langle \sigma \cdot v \rangle$$

$$MACS \equiv \frac{\langle \sigma \cdot v \rangle}{v_T} = \frac{2}{\sqrt{\pi}(kT)^2} \int_0^\infty \sigma(E) E e^{-E/(kT)} dE$$

Two methods are used to determine MACS:

1. measurement of **energy dependent** neutron capture cross-sections;
2. **integral measurement** (energy integrated) using neutron beams with suitable energy spectrum.

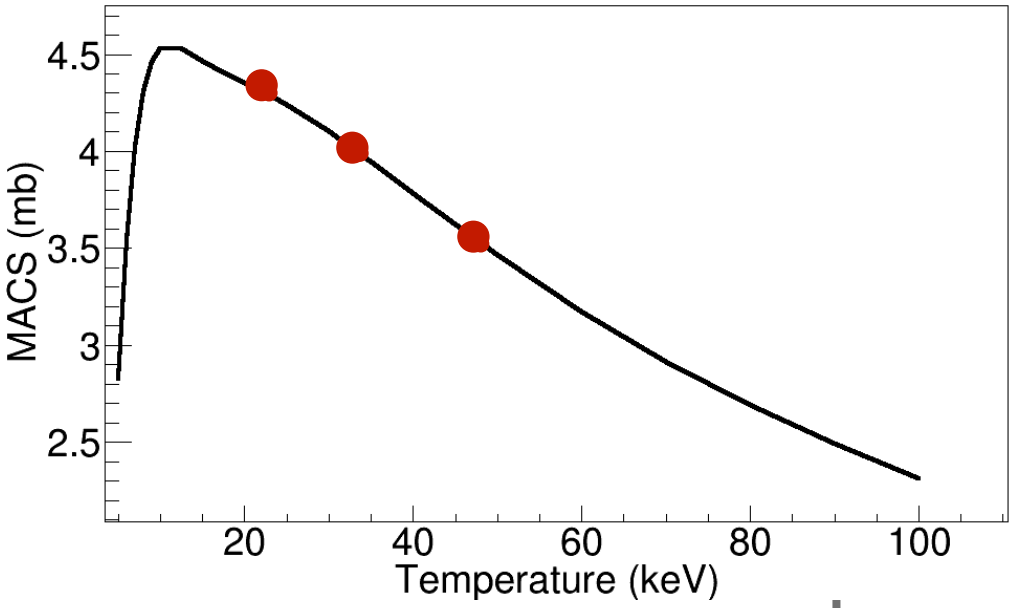

The n_TOF project

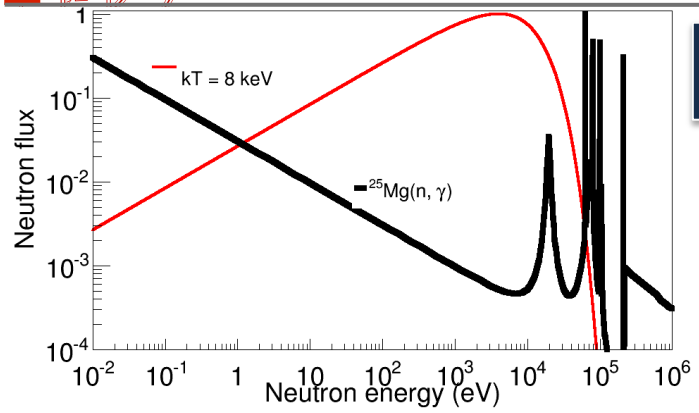

For Astrophysical applications it is important to determine **Maxwellian Averaged Cross-Sections (MACS)**, for various temperatures (kT depends on stellar site).

Reaction rate ($cm^{-3}s^{-1}$): $r = N_A N_n v\sigma(v)$

$$\rightarrow r = N_A N_n \langle \sigma \cdot v \rangle$$

$$MACS \equiv \frac{\langle \sigma \cdot v \rangle}{v_T} = \frac{2}{\sqrt{\pi}(kT)^2} \int_0^\infty \sigma(E) E e^{-E/(kT)} dE$$

Two methods are used to determine MACS:

1. measurement of **energy dependent** neutron capture cross-sections;

n_TOF @ CERN

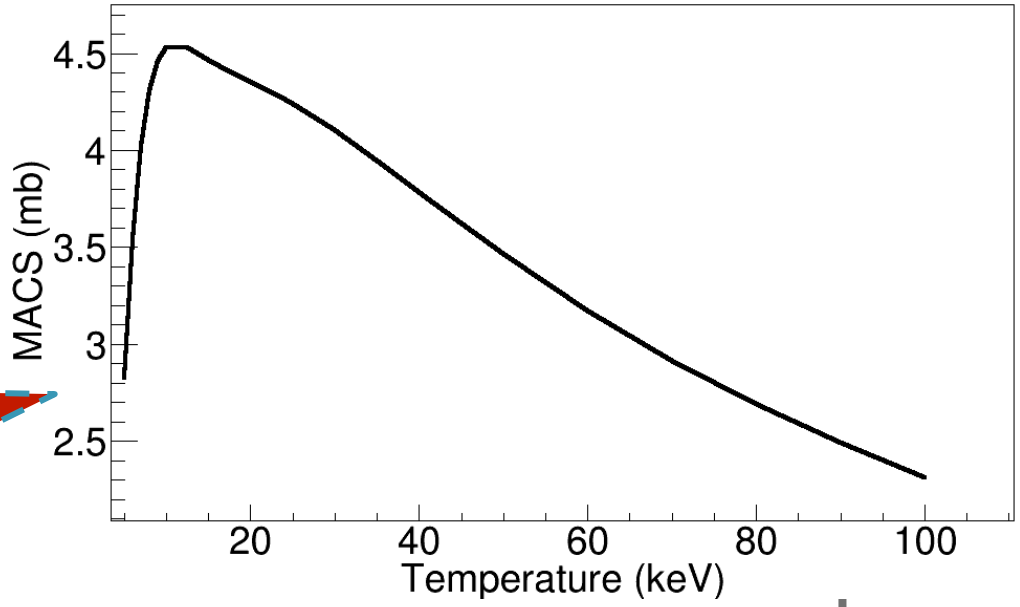

The n_TOF project

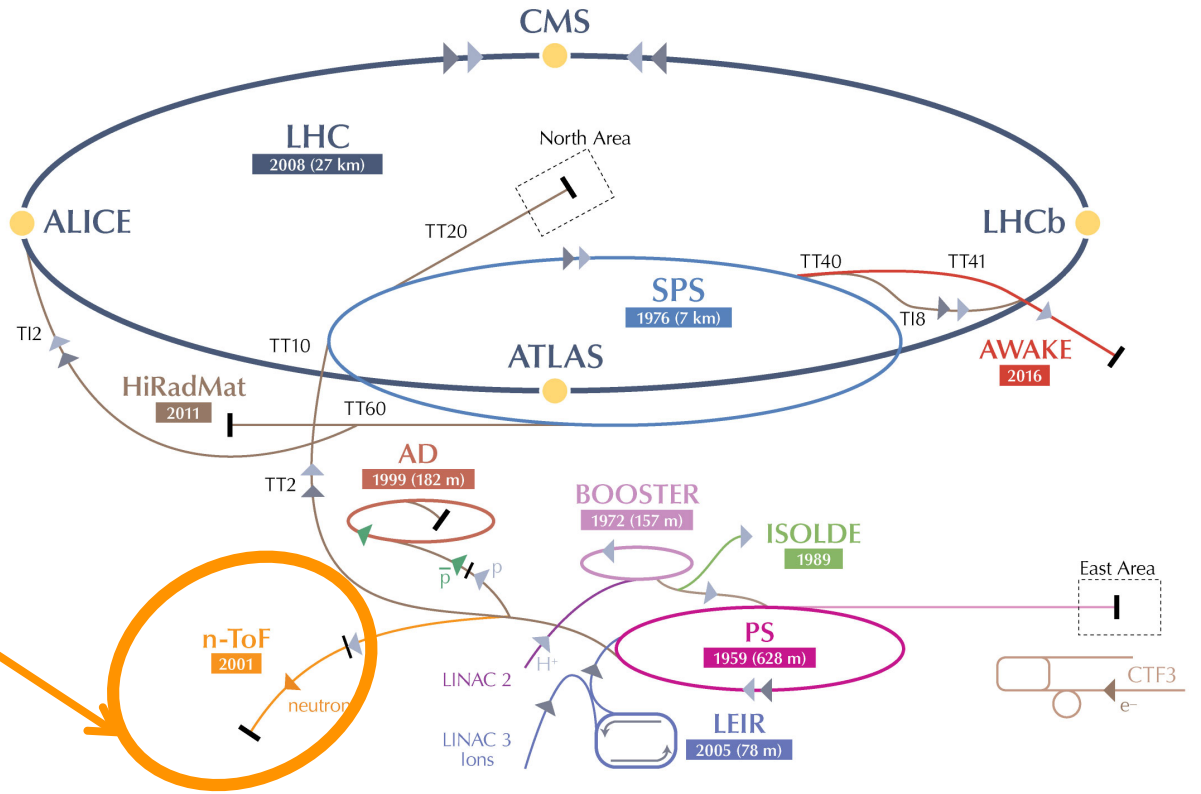

Neutron Time-Of- Flight facility: **n_TOF**

The n_TOF project

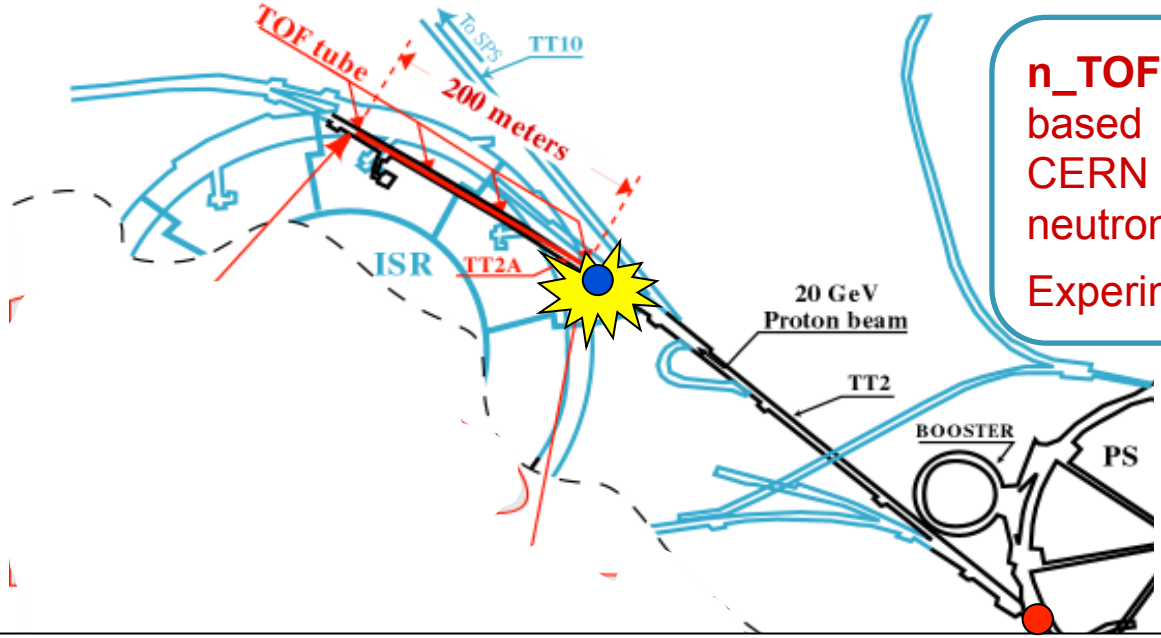

n_TOF is a **spallation** neutron source based on **20 GeV/c protons** from the CERN PS hitting a **Pb block** (~300 neutrons per proton and ~ 7×10^{12} ppp).

Experimental area at **185 m** and **18.5 m**.

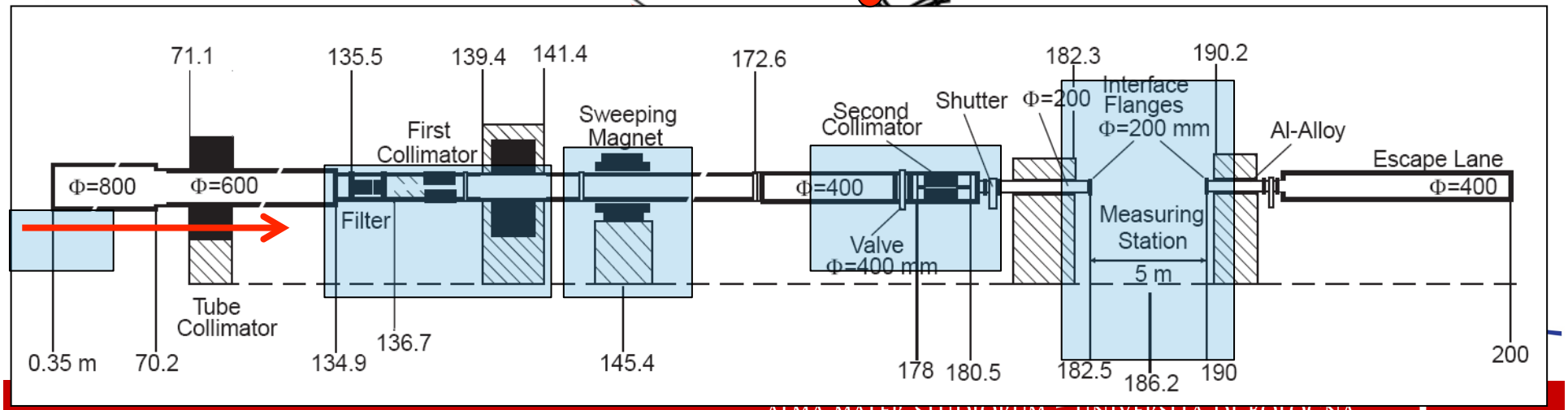

The n_TOF project

The advange of n_TOF are a direct consequence of the characteristics of the **PS proton beam**: **high energy, high peak current, low duty cycle.**

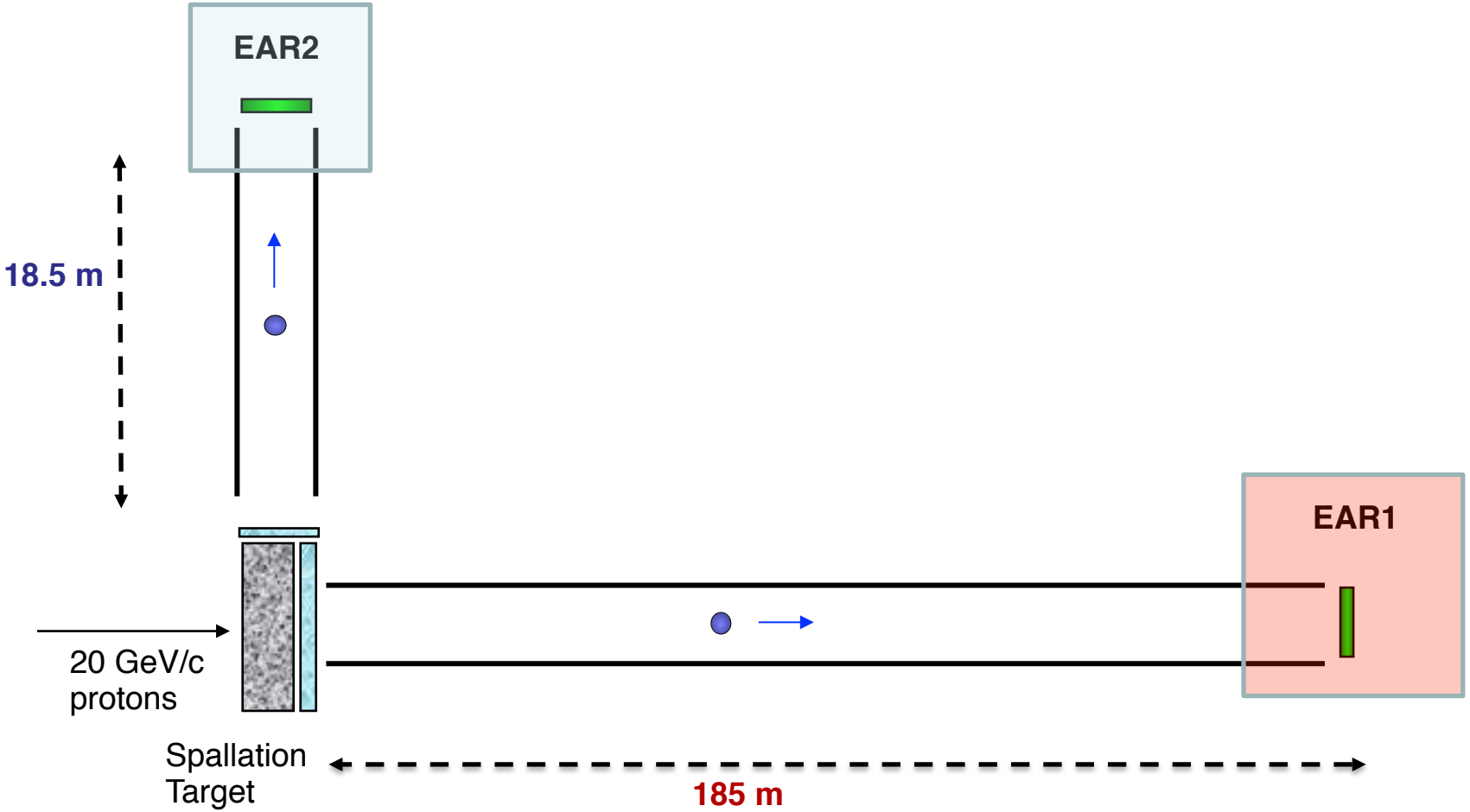

The n_TOF project

The advange of n_TOF are a direct consequence of the characteristics of the **PS proton beam**: **high energy, high peak current, low duty cycle.**

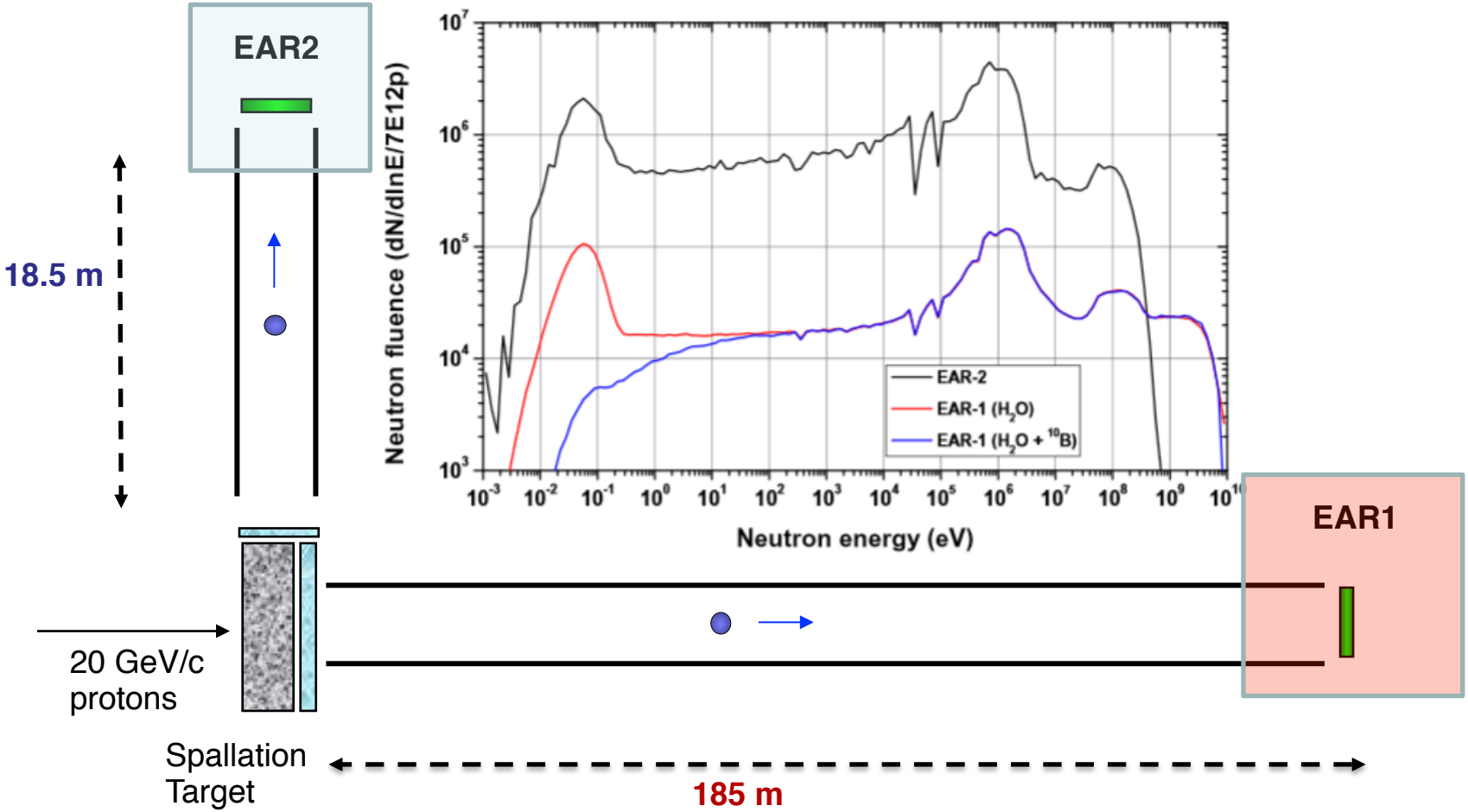

The n_TOF project

The advange of n_TOF are a direct consequence of the characteristics of the **PS proton beam**: **high energy, high peak current, low duty cycle.**

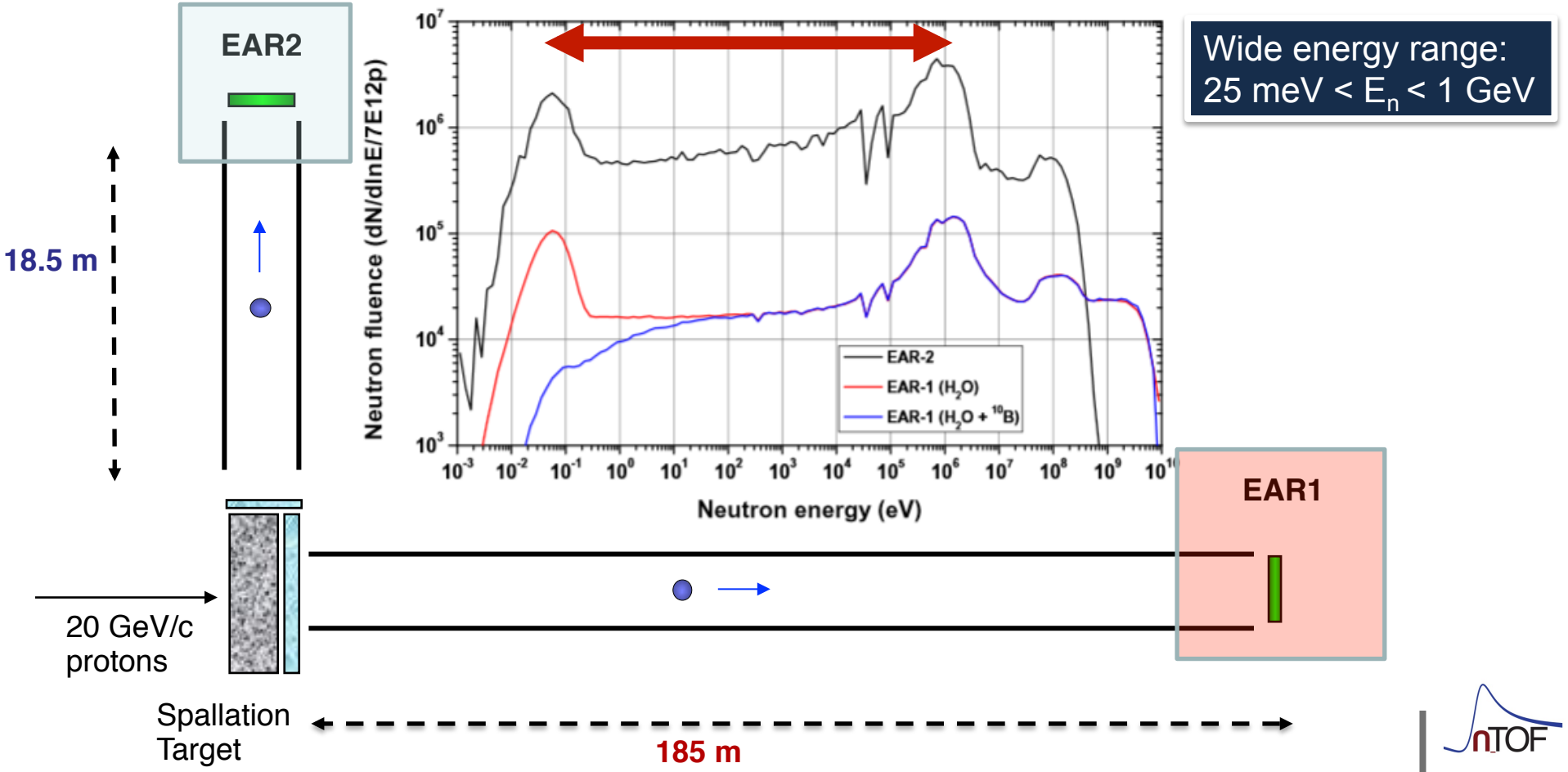

The n_TOF project

The advange of n_TOF are a direct consequence of the characteristics of the **PS proton beam**: **high energy, high peak current, low duty cycle.**

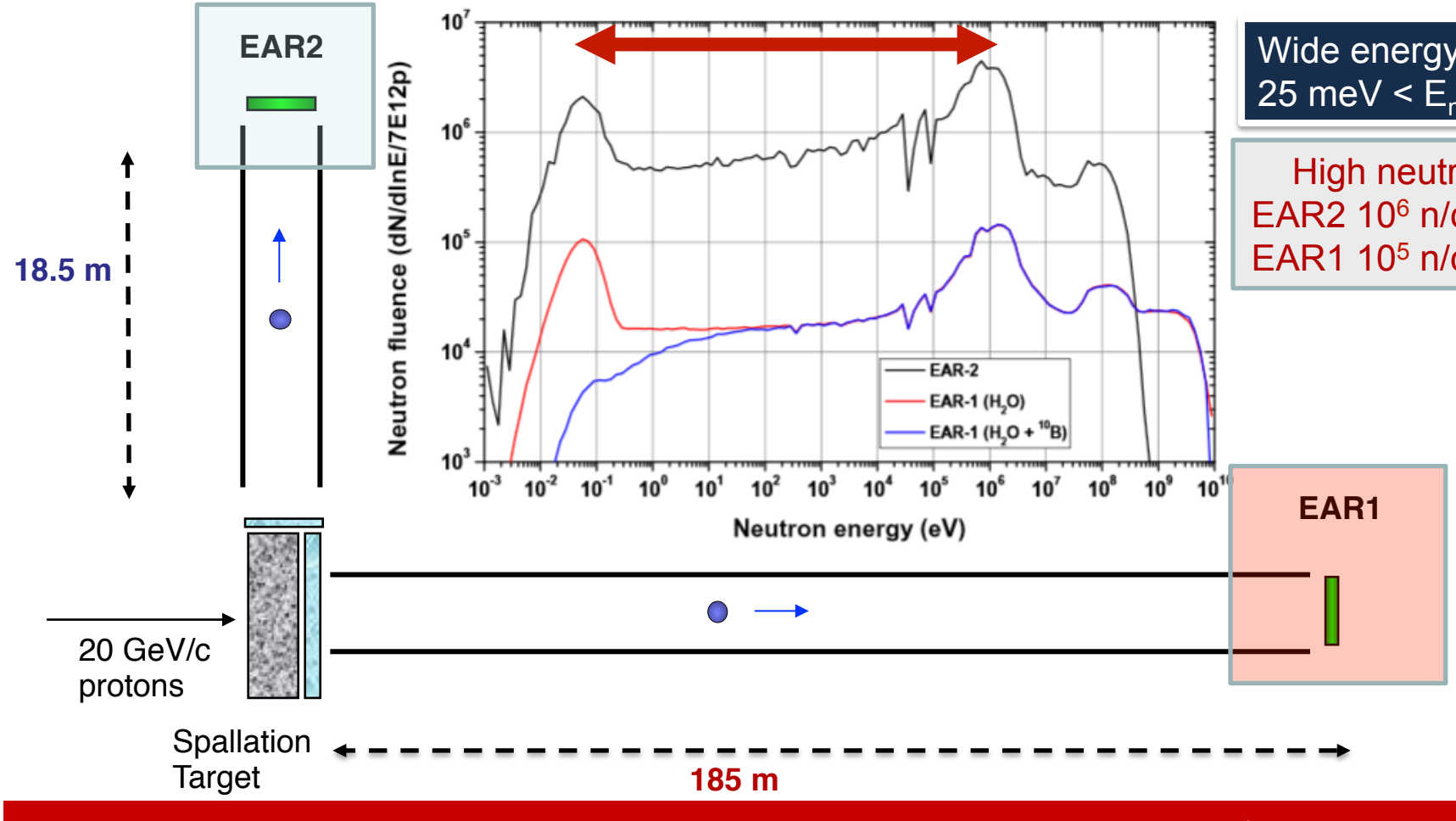

Wide energy range:
25 meV < E_n < 1 GeV

High neutron flux
EAR2 10^6 n/cm^2/pulse
EAR1 10^5 n/cm^2/pulse

The n_TOF project

The advange of n_TOF are a direct consequence of the characteristics of the **PS proton beam**: **high energy, high peak current, low duty cycle.**

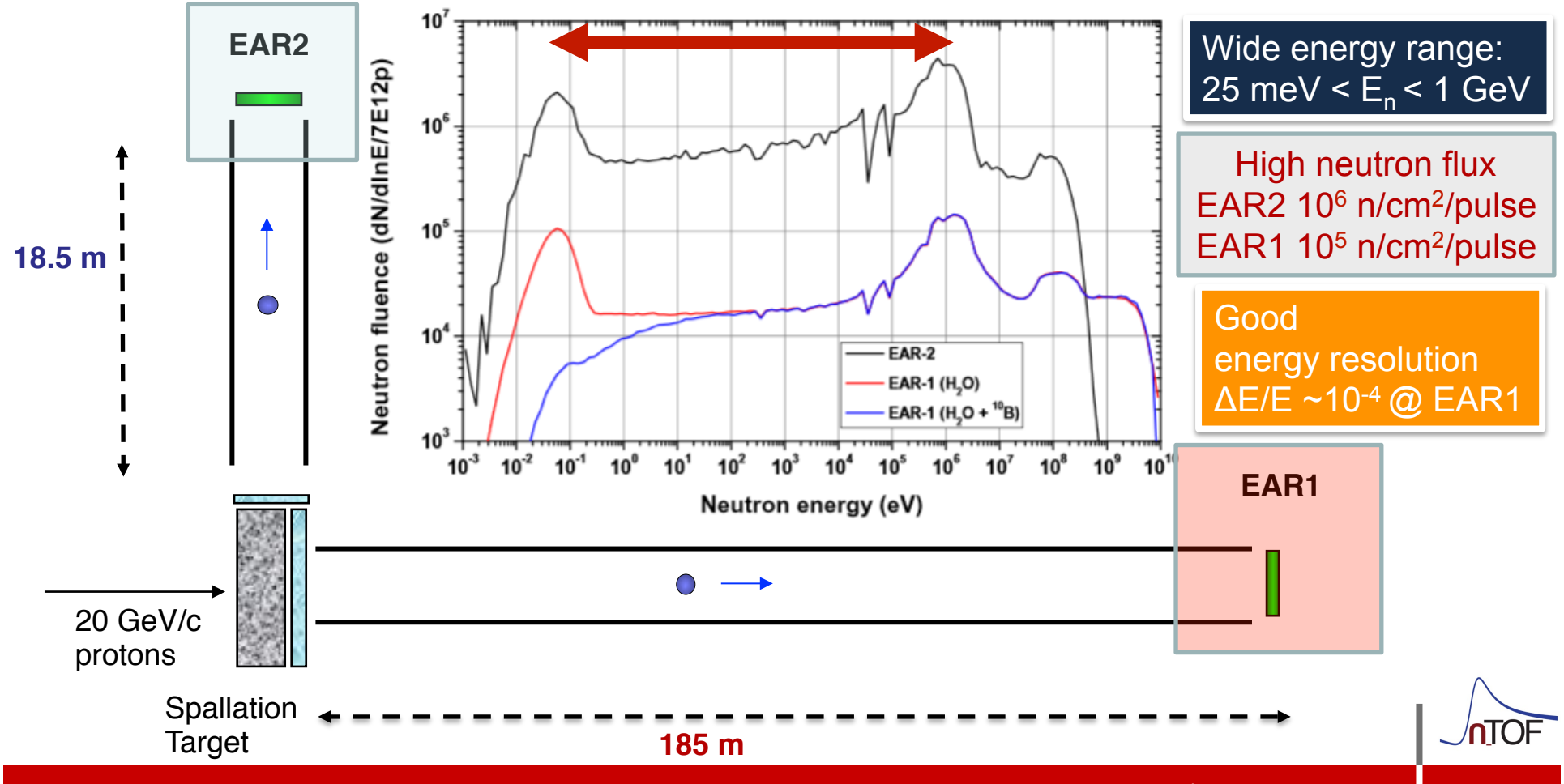

Wide energy range:
25 meV < E_n < 1 GeV

High neutron flux
EAR2 10^6 n/cm^2/pulse
EAR1 10^5 n/cm^2/pulse

Good
energy resolution
$\Delta E/E \sim 10^{-4}$ @ EAR1

The n_TOF project

Detectors for (n,γ) reaction

Capture reactions are measured by detecting γ-rays emitted in the de-excitation process. **Two different systems**, to minimize different types of background

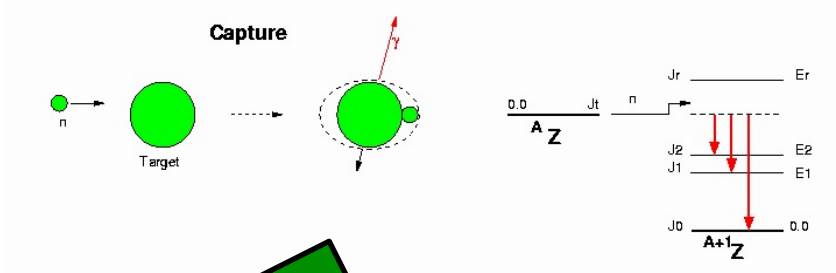

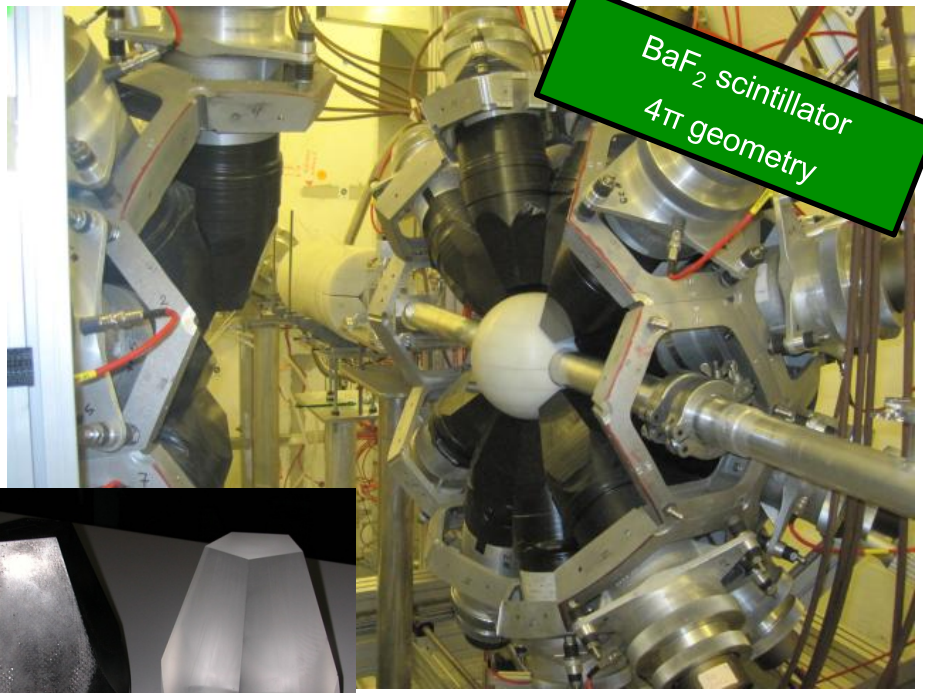

The n_TOF project

Detectors: (n,p) and (n,α) reactions

Gas and solid state detectors are used for detecting charged particles, depending on the energy region of interest and the Q-value of the reaction

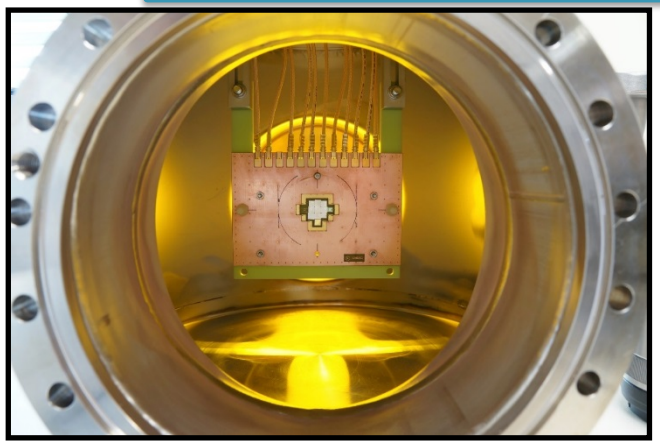

Silicon detectors
Silicon sandwich
Diamond detector
ΔE-E Telescopes

Micromegas chamber

- low-noice, high-gain, radiation-hard detector

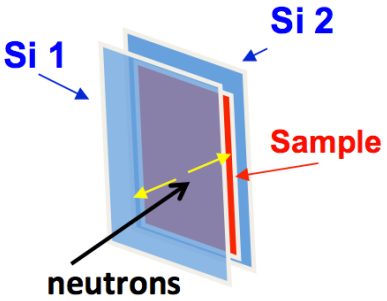

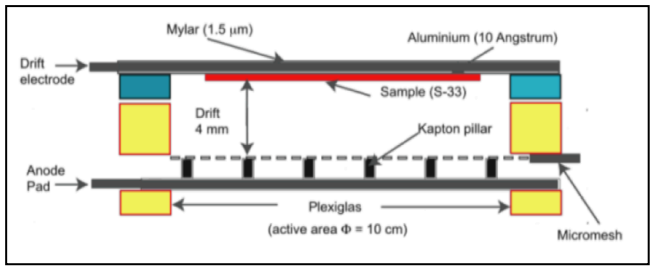

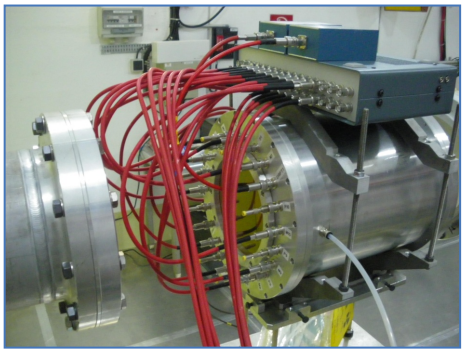

Data for s process

Cross sections measured in 2001 - 2018

- Branching point isotopes:

  ^{151}Sm, ^{63}Ni, ^{147}Pm, ^{171}Tm, ^{203}Tl

- Abundances in presolar grains:

  ^{91,92,93,94,96}Zr

- Magic Nuclei and end-point:

  ^{139}La, ^{140}Ce, ^{90}Zr, ^{89}Y, ^{88}Sr, ^{204,206,207,208}Pb, ^{209}Bi

- Seeds isotopes:

  ^{54,56,57}Fe, ^{58,60,62}Ni, ^{59}Ni(n,α)

- Isotopes of special interest:

  ^{186,187,188}Os (cosmochronometer),^{197}Au (reference cross section), ^{24,25,26}Mg, ^{33}S(n,α), ^{14}N(n,p), ^{35}Cl(n,p), ^{26}Al(n,p), ^{26}Al(n,α) (neutron poison), ^{154}Gd (s-only isotope), ^{68}Zn, ^{69,71}Ga, ^{70,72,73,74,76}Ge, ^{77,78,80}Se (weak component)

- Neutron Sources ^{22}Ne(α,n)^{25}Mg and ^{13}C(α,n)^{16}O:

  n+^{25}Mg, n+^{16}O

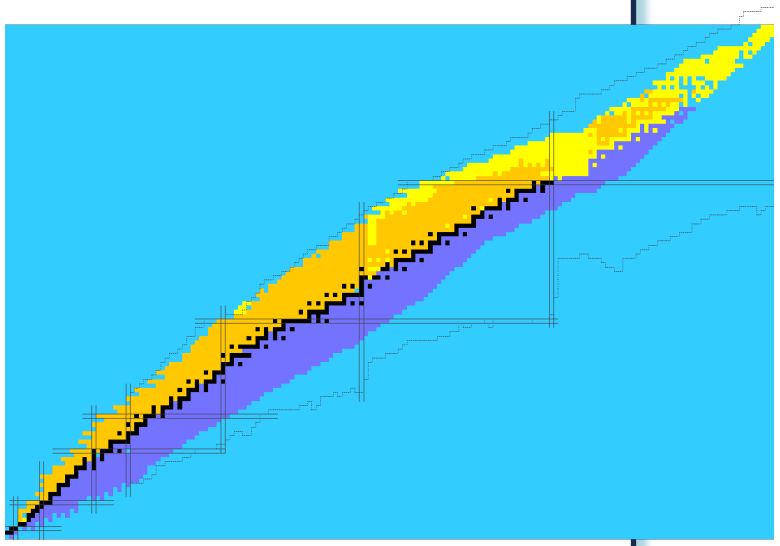

Data for s process

Cross sections measured in 2001 - 2018

- Branching point isotopes:

  ^{151}Sm, ^{63}Ni, ^{147}Pm, ^{171}Tm, ^{203}Tl

  The neutron capture cross section measurement of the thallium isotopes ^{203}Tl, ^{204}Tl and ^{205}Tl at the n_TOF facility at CERN, A. Casanovas

- Abundances in presolar grains:

  ^{91,92,93,94,96}Zr

@ NICXV

- Magic Nuclei and end-point:

  ^{139}La, ^{140}Ce, ^{90}Zr, ^{89}Y, ^{88}Sr, ^{204,206,207,208}Pb, ^{209}Bi

- Seeds isotopes:

  ^{54,56,57}Fe, ^{58,60,62}Ni, ^{59}Ni(n,α)

  The Stellar ^{72}Ge(n,γ) Cross Section: A First Measurement at n_TOF, M. Dietz

- Isotopes of special interest:

  ^{186,187,188}Os (cosmochronometer), ^{197}Au (reference cross section), ^{24,25,26}Mg, ^{33}S(n,α), ^{14}N(n,p), ^{35}Cl(n,p), ^{26}Al(n,p), ^{26}Al(n,α) (neutron poison), ^{154}Gd (s-only isotope), ^{68}Zn, ^{69,71}Ga, ^{70,72,73,74,76}Ge, ^{77,78,80}Se (weak component)

- Neutron Sources ^{22}Ne(α,n)^{25}Mg and ^{13}C(α,n)^{16}O:

  n+^{25}Mg, n+^{16}O

  Measurement of the ^{16}O(n,α)^{13}C reaction cross-section at the CERN n_TOF facility – S. Urlass

Branching point isotopes

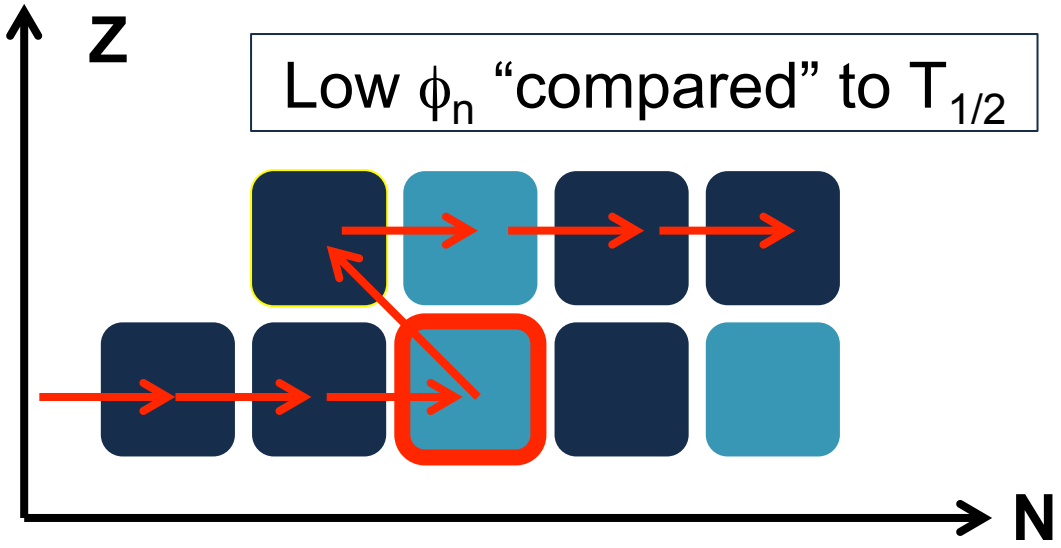

STABLE

Unstable against β^-

(n,γ) reaction

β^- decay

Branching point isotopes

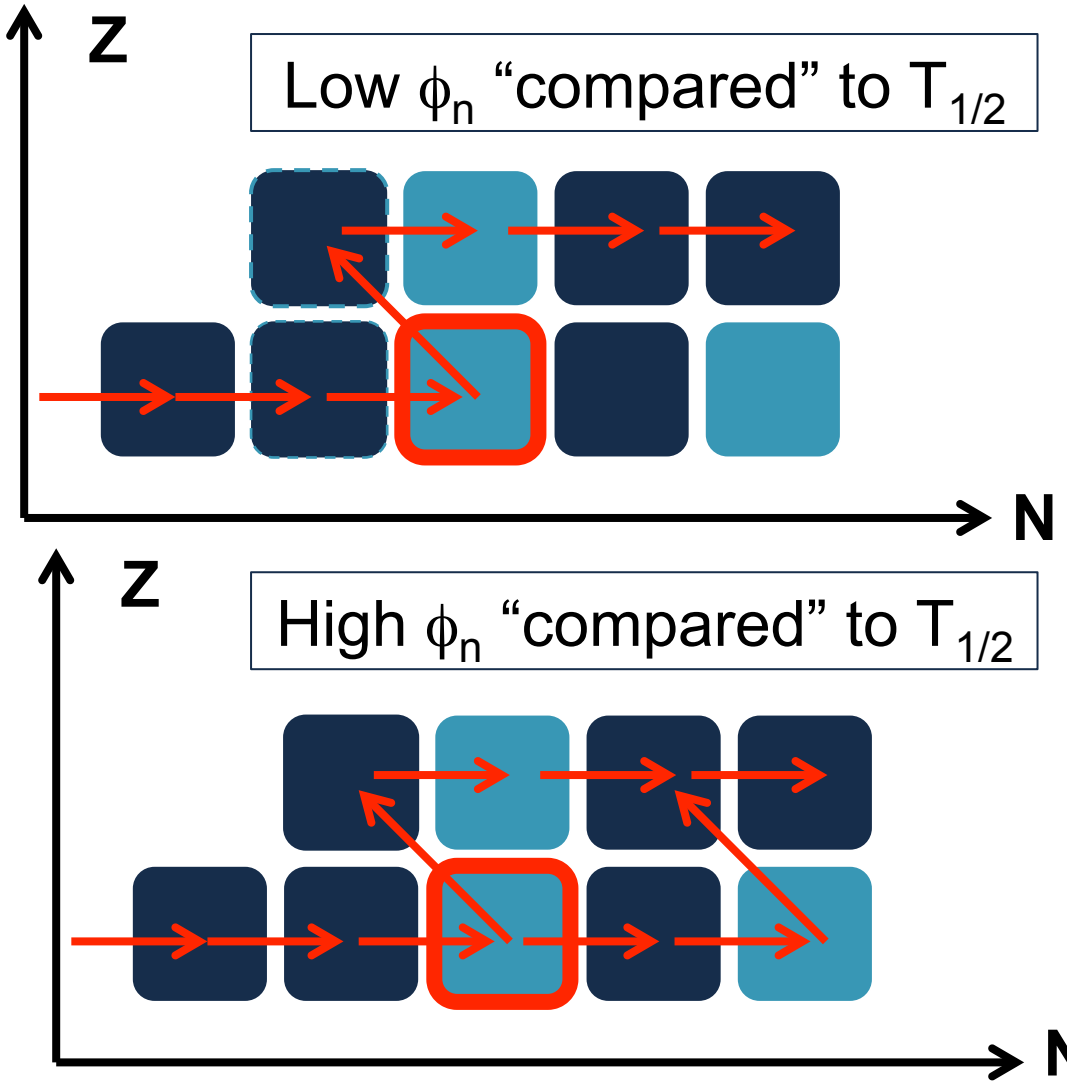

STABLE

Unstable against β^-

(n,γ) reaction

β^- decay

s-process branching point

^{151}Sm: s process in AGB

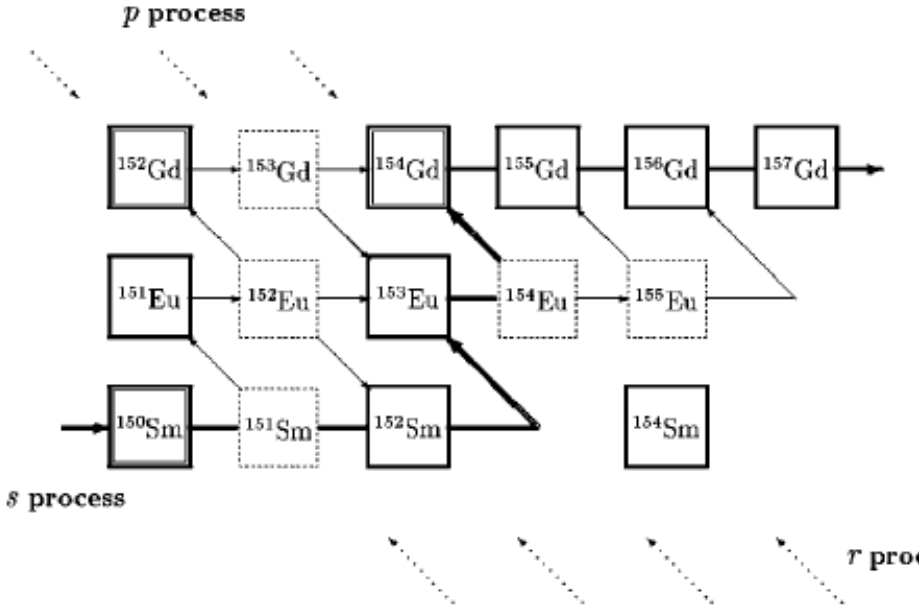

Phys. Rev. Lett. **93**, 161103 (2004)

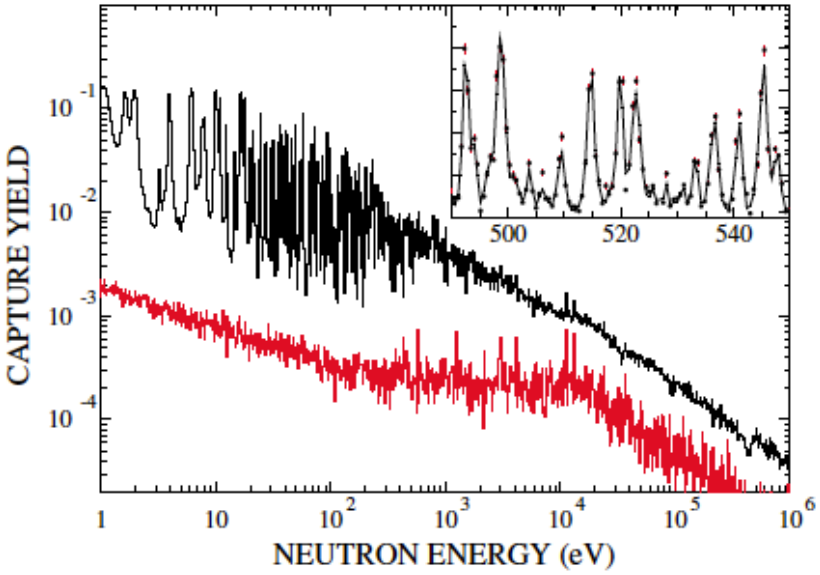

$$f_\beta = \frac{(\langle\sigma\rangle N)_{^{152}\mathrm{Gd}}}{(\langle\sigma\rangle N)_{^{150}\mathrm{Sm}}} = \frac{\lambda_{^{151}\mathrm{Sm}}}{\lambda_{^{151}\mathrm{Sm}} + n_n \langle\sigma v\rangle_{^{151}\mathrm{Sm}}}$$

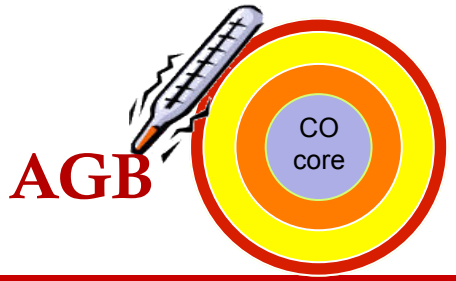

<σ> = 3.1±0.16 b
at kT=30 keV

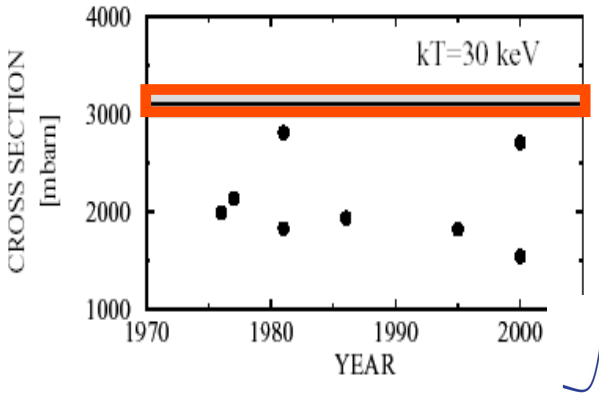

Branching point isotopes

REVIEWS OF MODERN PHYSICS The s process: Nuclear physics, stellar models, and observations, Vol. 83, 2011

Sample	Half-life (yr)	Q value (MeV)	Comment
^{63}Ni	100.1	β^-, 0.066	TOF work in progress (Couture, 2009), sample with low enrichment
^{79}Se	2.95×10^5	β^-, 0.159	Important branching, constrains s-process temperature in massive stars
^{81}Kr	2.29×10^5	EC, 0.322	Part of ^{79}Se branching
^{85}Kr	10.73	β^-, 0.687	Important branching, constrains neutron density in massive stars
^{95}Zr	64.02 d	β^-, 1.125	Not feasible in near future, but important for neutron density low-mass AGB stars
^{134}Cs	2.0652	β^-, 2.059	Important branching at $A = 134, 135$, sensitive to s-process temperature in low-mass AGB stars, measurement not feasible in near future
^{135}Cs	2.3×10^6	β^-, 0.269	So far only activation measurement at $kT = 25$ keV by Patronis *et al.* (2004)
^{147}Nd	10.981 d	β^-, 0.896	Important branching at $A = 147/148$, constrains neutron density in low-mass AGB stars
^{147}Pm	2.6234	β^-, 0.225	Part of branching at $A = 147/148$
^{148}Pm	5.368 d	β^-, 2.464	Not feasible in the near future
^{151}Sm	90	β^-, 0.076	Existing TOF measurements, full set of MACS data available (Abbondanno *et al.*, 2004a; Wisshak *et al.*, 2006c)
^{154}Eu	8.593	β^-, 1.978	Complex branching at $A = 154, 155$, sensitive to temperature and density
^{155}Eu	4.753	β^-, 0.246	So far only activation measurement at $kT = 25$ keV by Jaag and Käppeler (1995)
^{153}Gd	0.658	EC, 0.244	Part of branching at $A = 154, 155$
^{160}Tb	0.198	β^-, 1.833	Weak temperature-sensitive branching, very challenging experiment
^{163}Ho	4570	EC, 0.0026	Branching at $A = 163$ sensitive to mass density during s process, so far only activation measurement at $kT = 25$ keV by Jaag and Käppeler (1996b)
^{170}Tm	0.352	β^-, 0.968	Important branching, constrains neutron density in low-mass AGB stars
^{171}Tm	1.921	β^-, 0.098	Part of branching at $A = 170, 171$
^{179}Ta	1.82	EC, 0.115	Crucial for s-process contribution to ^{180}Ta, nature's rarest stable isotope
^{185}W	0.206	β^-, 0.432	Important branching, sensitive to neutron density and s-process temperature in low-mass AGB stars
^{204}Tl	3.78	β^-, 0.763	Determines ^{205}Pb/^{205}Tl clock for dating of early Solar System

PRL 110, 022501 (2013)

PRL 93, 161103 (2004)

Branching point isotopes

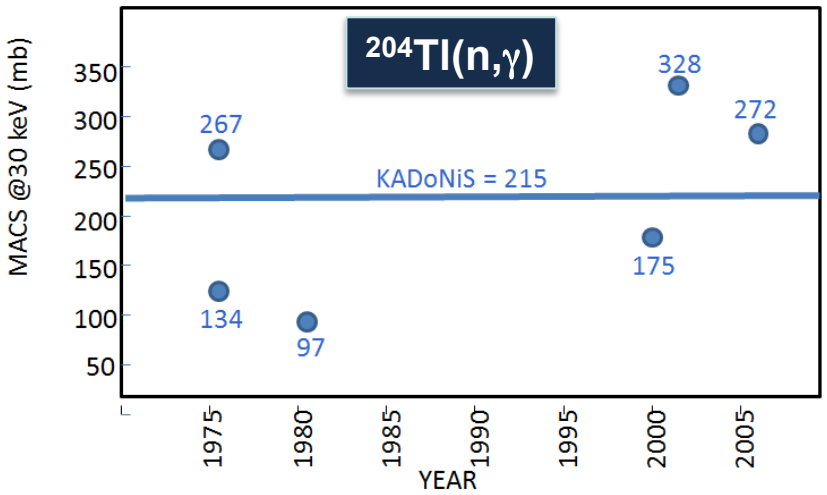

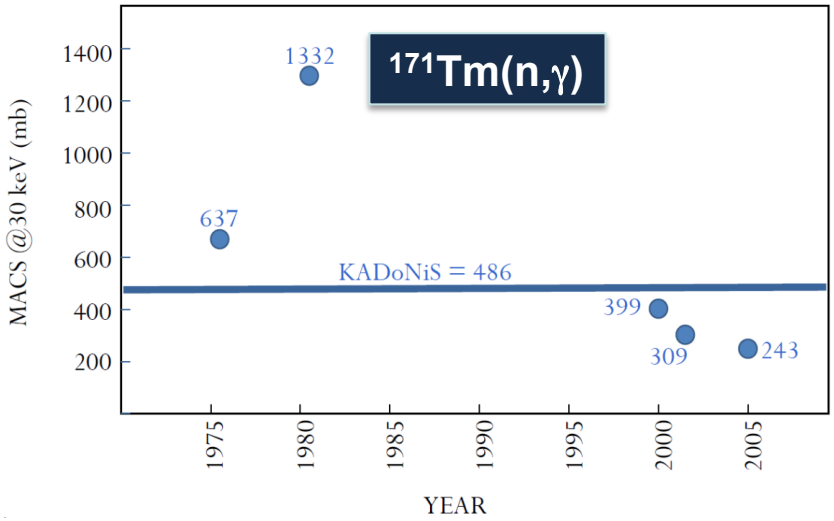

Ongoing studies

Short-lived branching isotopes (a few years) have either **never been measured before** or have been measured **only by activation** (a few tens of ng) at a fixed temperature.

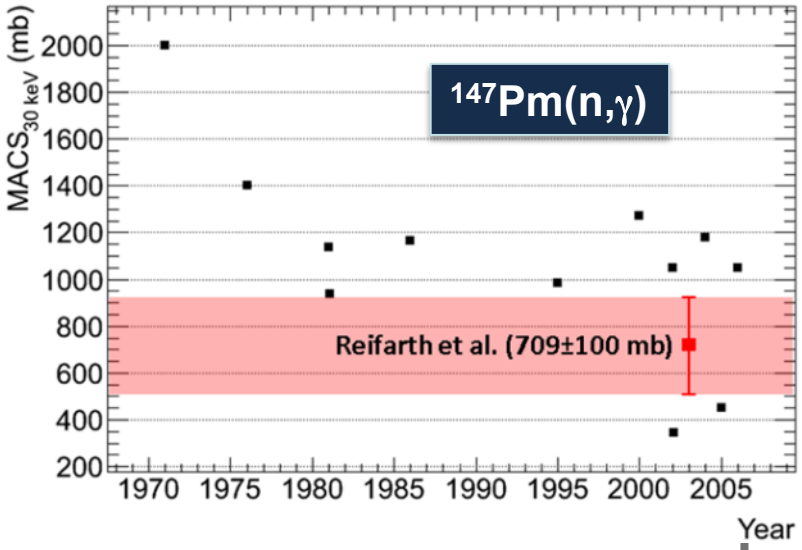

s-only isotopes

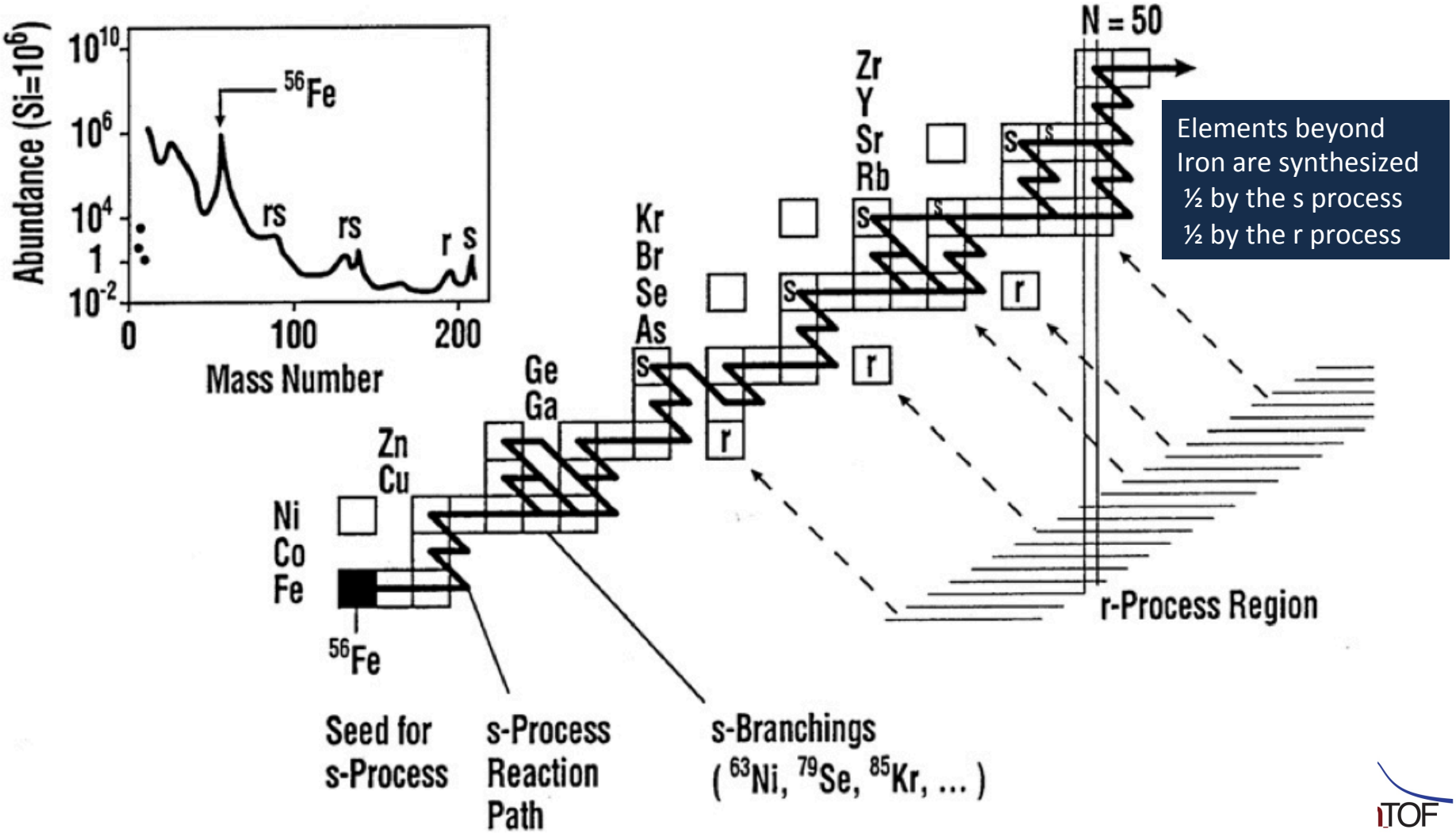

s-only isotopes

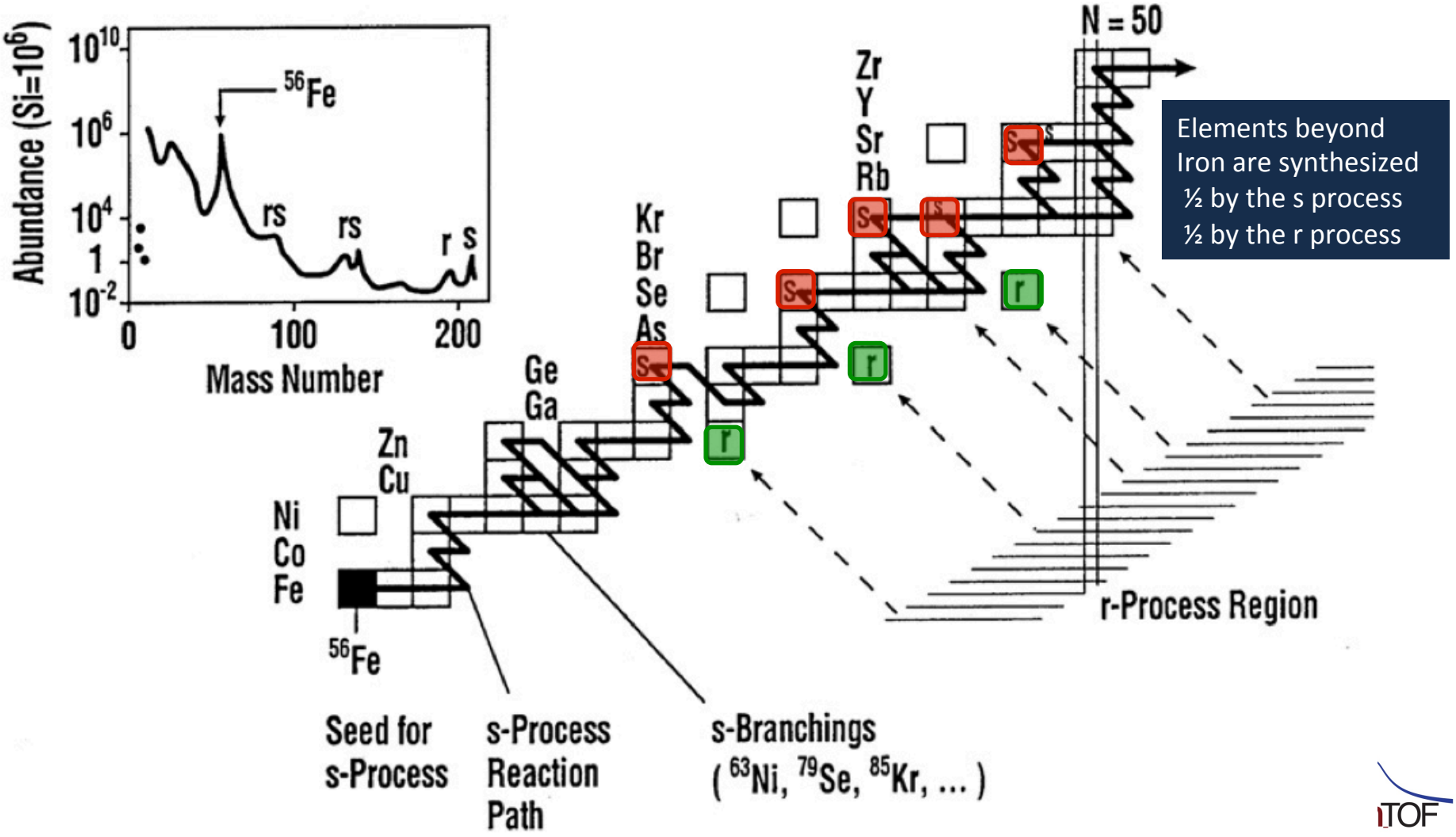

Elements beyond Iron are synthesized
½ by the s process
½ by the r process

s-only isotopes

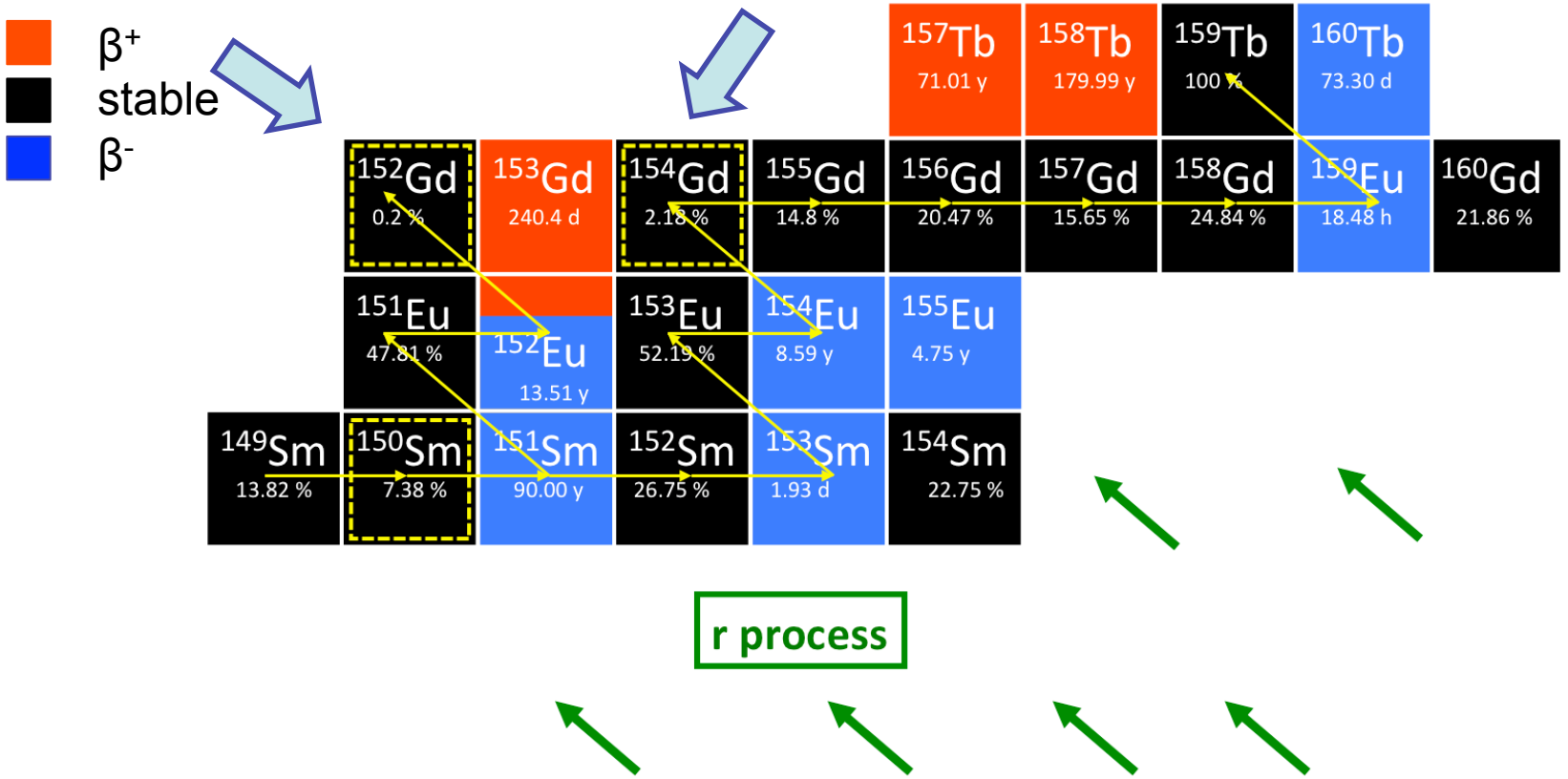

^{154}Gd = s-only isotope, it can be produced only via s process because they are shielded against the β-decay chains from the r-process region by the isobars samarium

s-only isotopes

3 very recent and **independent** studies:

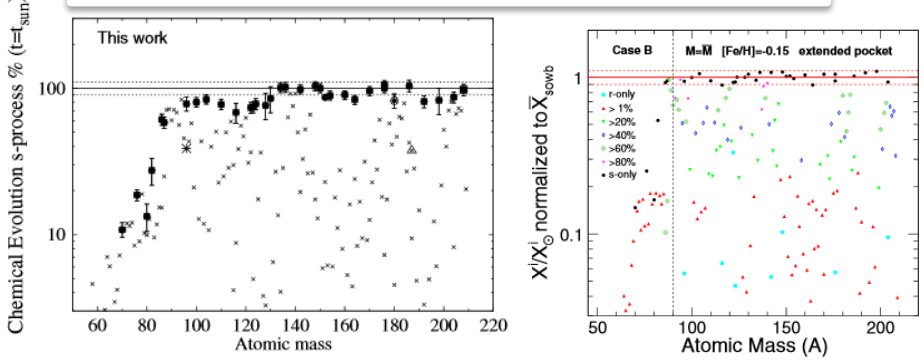

S. Bisterzo, *et al.*, The Astrophysical Journal **787** (2014) 10

C. Trippella, *et al.*, The Astrophysical Journal **787** (2014) 41

S. Cristallo, *et al.*, The Astrophysical Journal **801** (2015) 53

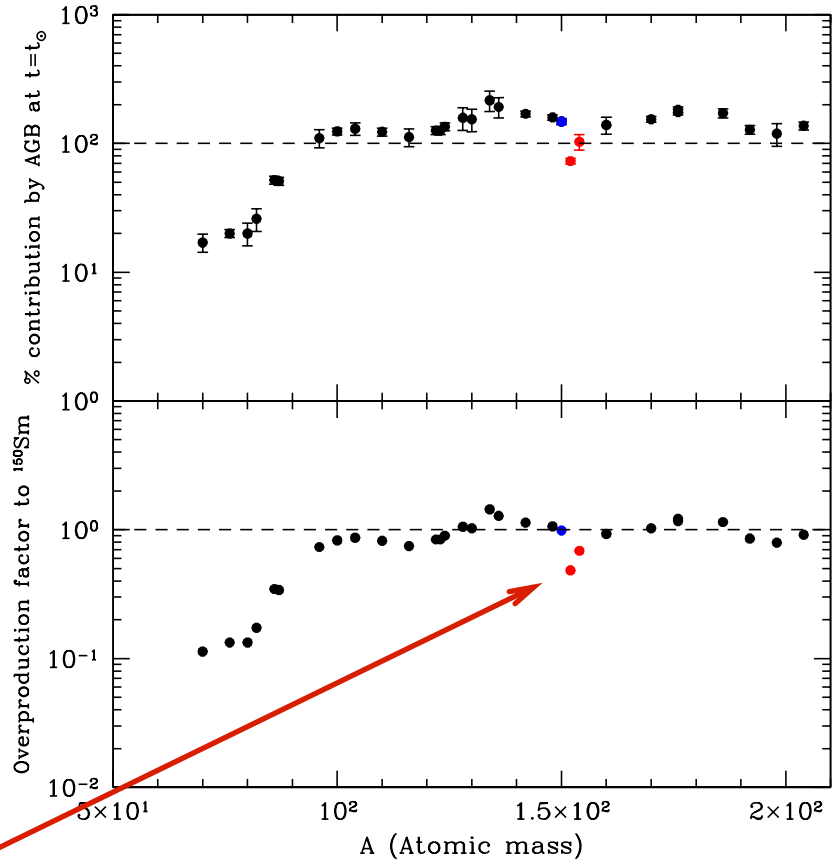

THE ASTROPHYSICAL JOURNAL, 801:53 (14pp), 2015 March 1

Disagreement of more than 20% between **observation** and **model calculation** of s-process abundances

s-only isotopes

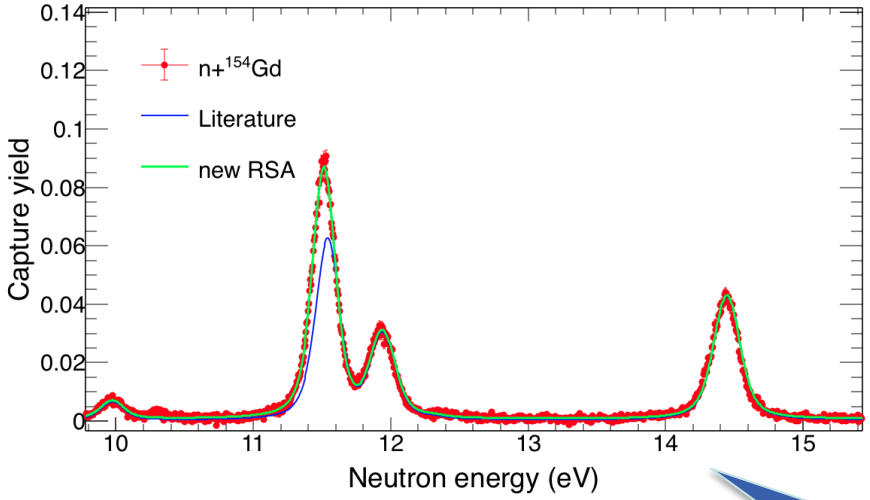

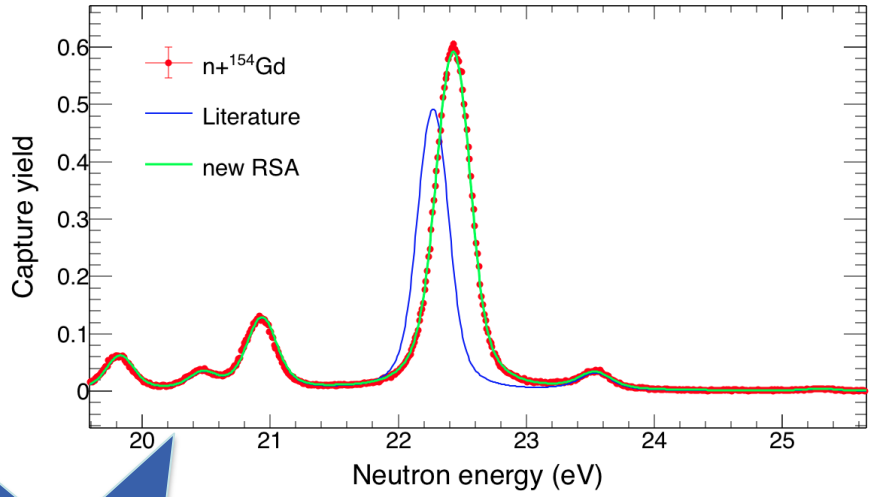

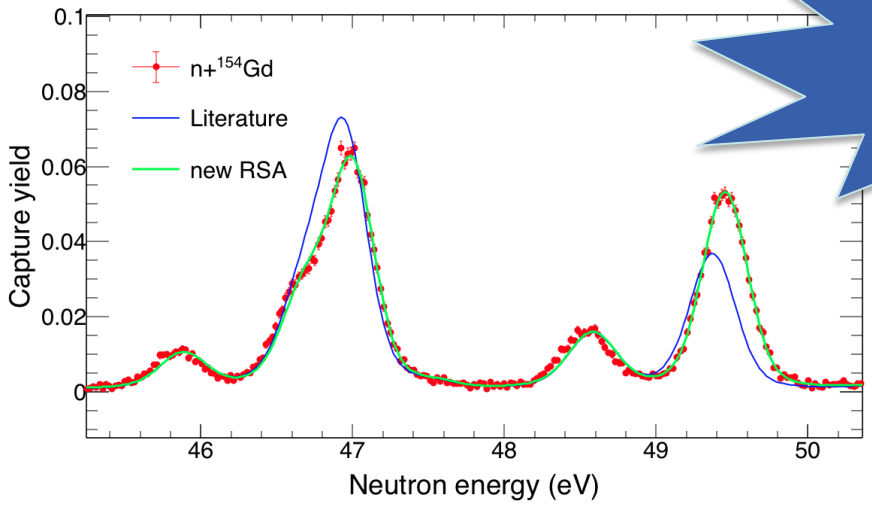

Measurement
August 2017

Preliminary R-Matrix analysis of ^{154}Gd(n,γ) seems to largely deviate from literature

Magic nuclei: s process peaks

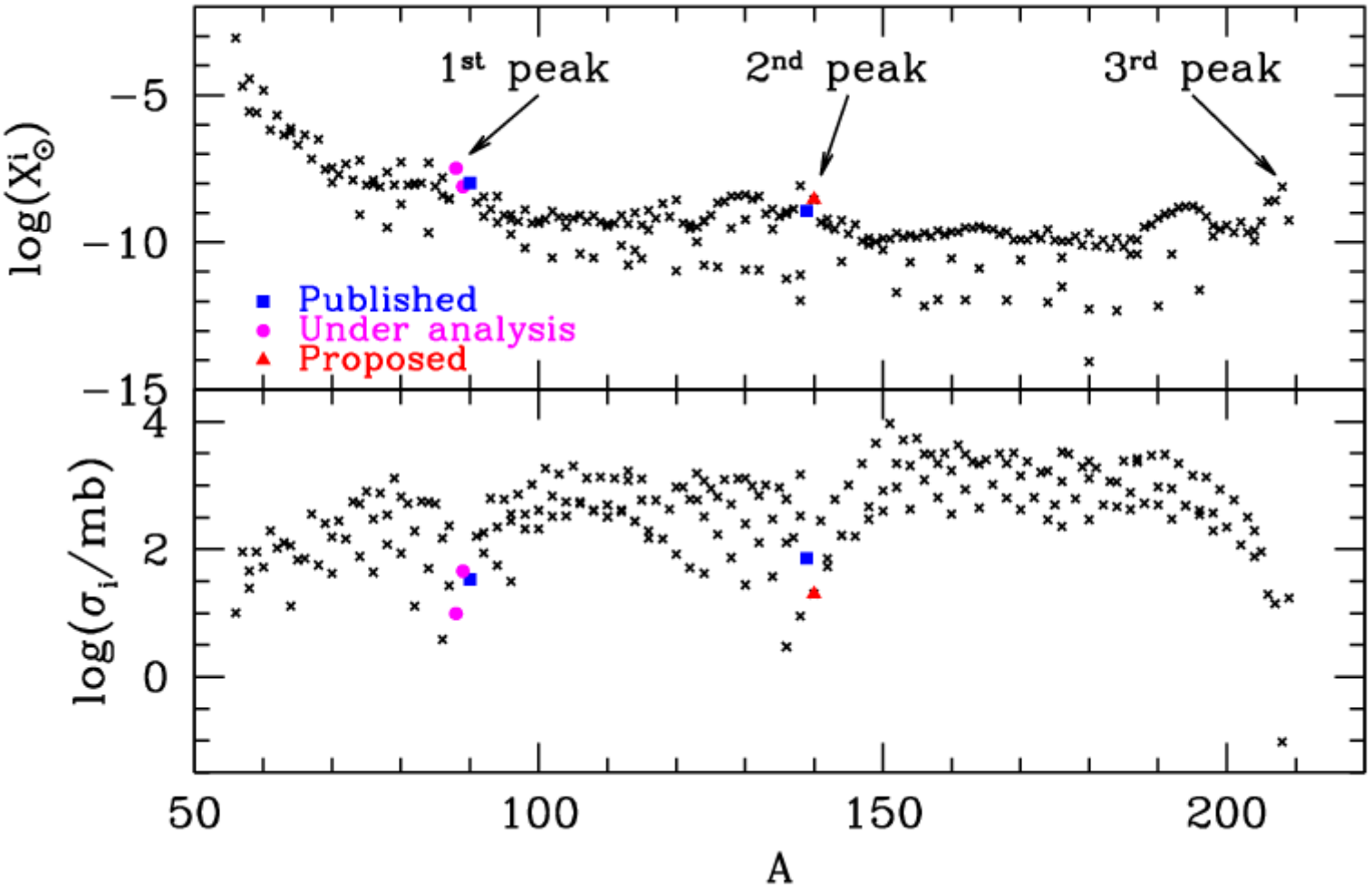

Magic nuclei: s process peaks

Straniero, Cristallo & Piersanti 2014

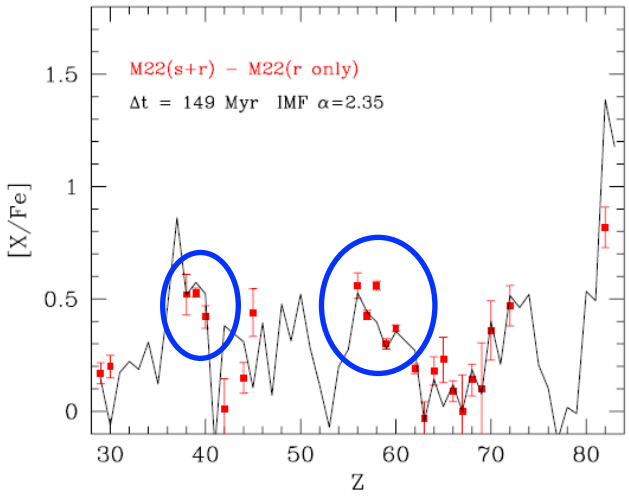

Figure 11. Best fit of the average *s*-process chemical pattern of stars in M22.

Abundances of elements in the **s-process peak** are well reproduced **apart** from **Cerium**.

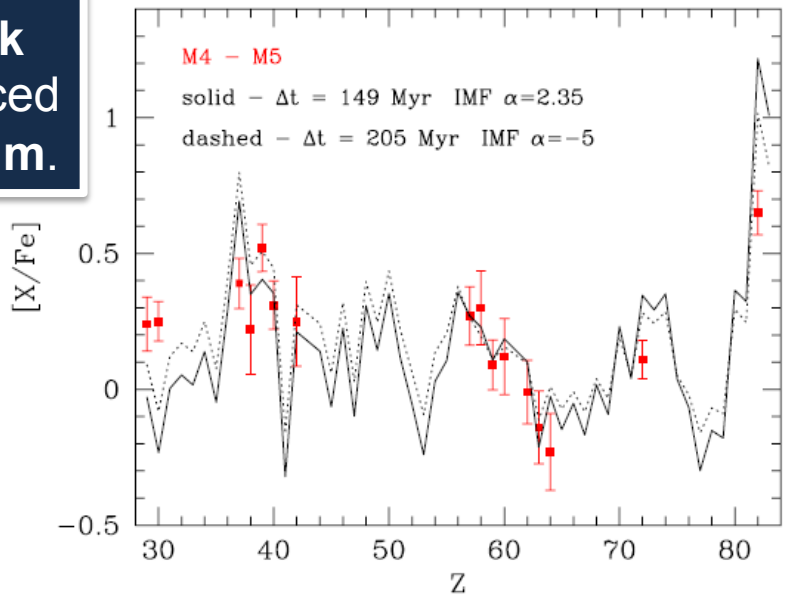

Figure 13. Best fit of the average *s*-process chemical pattern of stars in M4.

The pollution of AGB stars with a mass ranging between 3 to 6 M_{SUN} may account for most of the features of the *s*-process enrichment of M4 and M22.

Globular Cluster

M22

M4

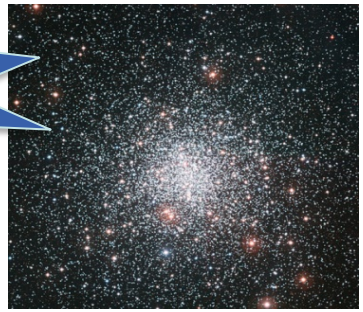

M5

Magic nuclei: s process peaks

^{140}Ce is the most abundant cerium isotope (88%)

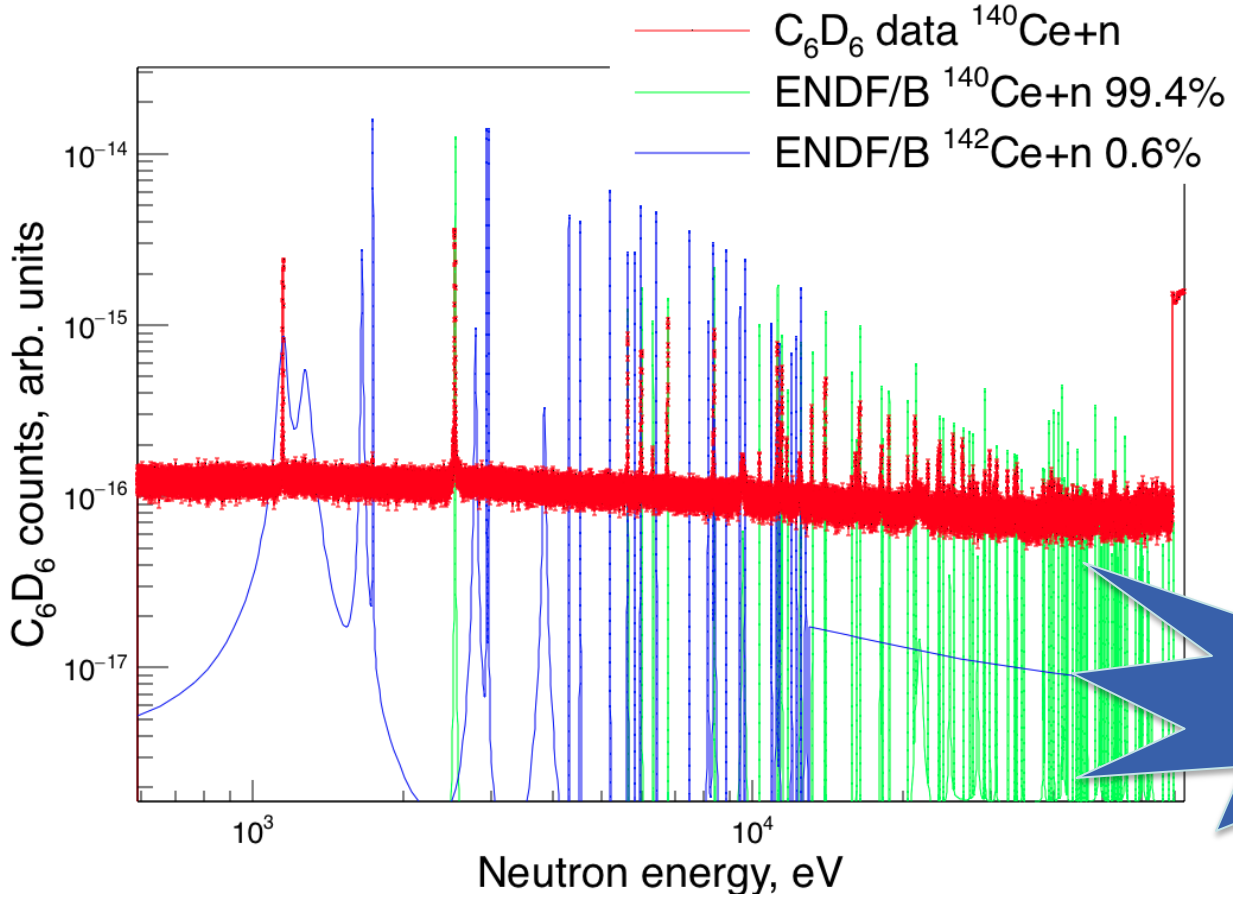

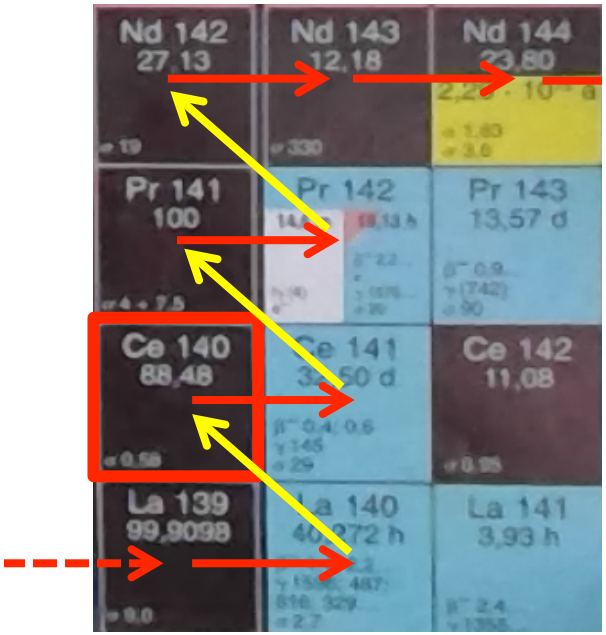

Measurement
May 2018

The case of ^{25}Mg

Constraints for the
^{22}Ne(α,n)^{25}Mg
^{22}Ne(α,γ)^{26}Mg
reactions

Experimental **evidence** of **natural spin parity** states in the energy region of interest

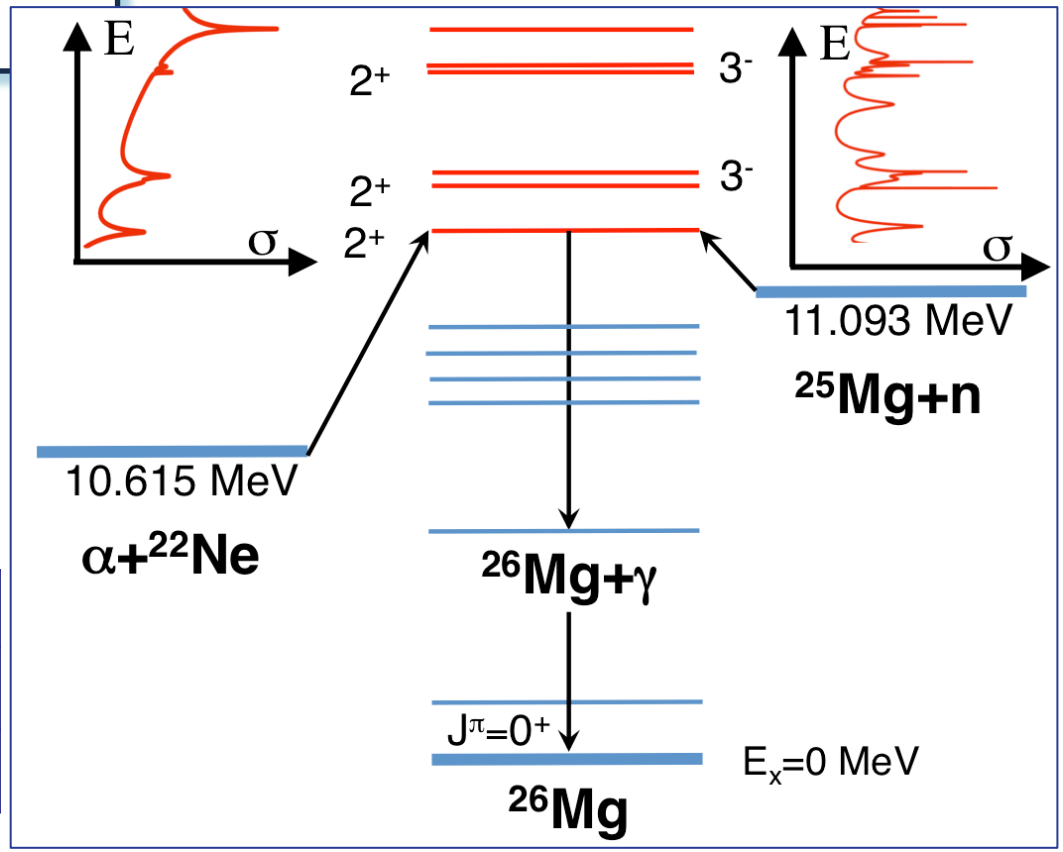

	J^π
^{22}Ne	0^+
α	0^+

	J^π
^{25}Mg	$5/2^+$
n	$1/2^+$

The case of ^{25}Mg

Constraints for the
^{22}Ne(α,n)^{25}Mg
^{22}Ne(α,γ)^{26}Mg
reactions

s abundance

M. Jaeger, PRL **87** (2001) 20

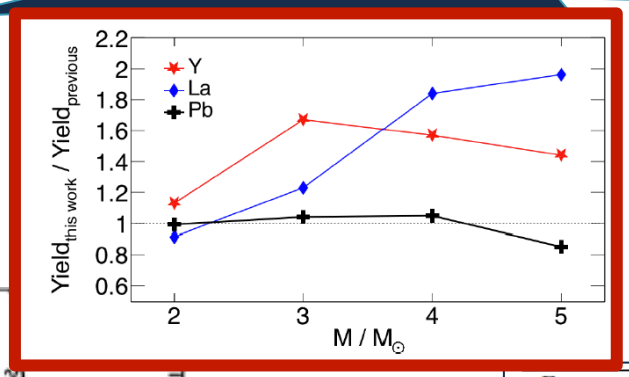

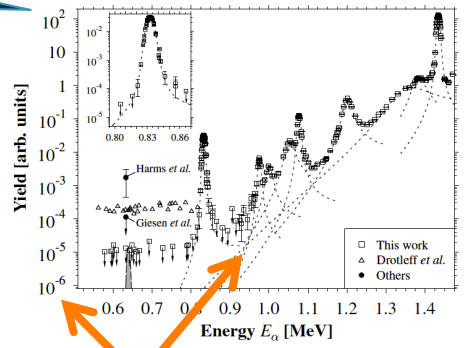

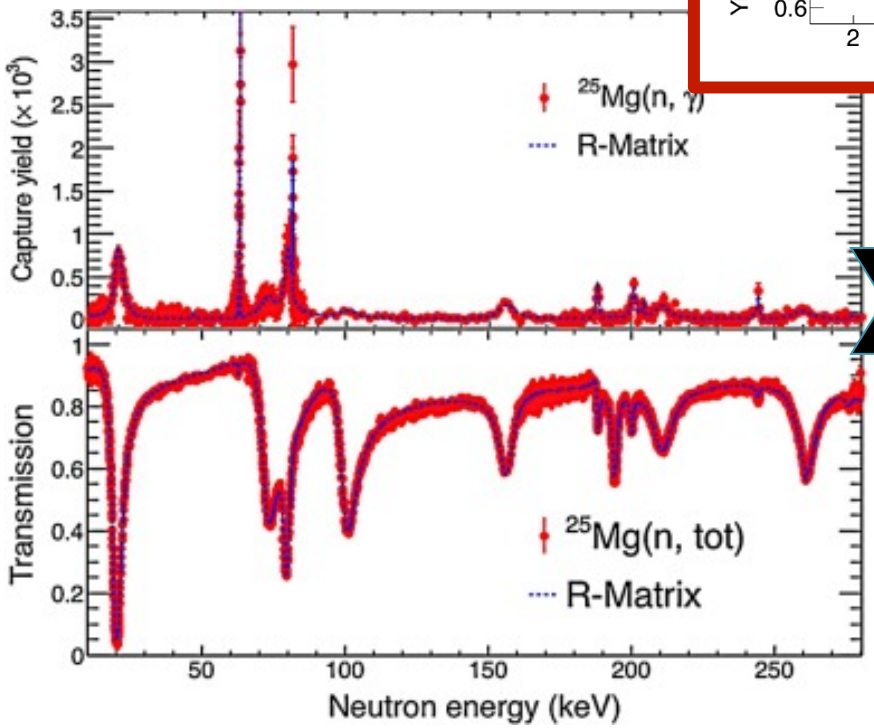

R-Matrix analysis

?

E_n (keV)	E_x (keV)	E_α^{Lab} (keV)	J^π ($\hbar$)	Γ_γ (eV)	Γ_n (eV)
19.92(1)	11112	589	2^+	1.37(6)	2095(5)
62.73(1)	11154		1^+	4.4(5)	7(2)
72.82(1)	11163	649	2^+	2.8(2)	5310(50)
79.23(1)	11169	656	$3^{-(a)}$	3.3(2)	1940(20)
81.11(1)	11171			5(1)	1 – 30
100.33(2)	11190		3^+	1.3(2)	5230(30)
155.83(2)	11243		2^-	4.7(5)	5950(50)
187.95(2)	11274	779	2^+	2.2(2)	410(10)
194.01(2)	11280	786	$3^{-(a)}$	0.3(1)	1810(20)
199.84(2)	11285		2^-	4.8(4)	1030(30)
203.88(4)	11289			0.9(3)	3 – 20
210.23(3)	11295		2^-	6.6(6)	7370(60)
243.98(2)	11328	843	$2^{+(b)}$	2.2(3)	171(6)
260.84(8)	11344			1.0(2)	300 – 3900
261.20(2)	11344		> 3	3.0(3)	6000 – 9000

Future 2021 - 2030

Upgrade: new spallation target ready by 2020

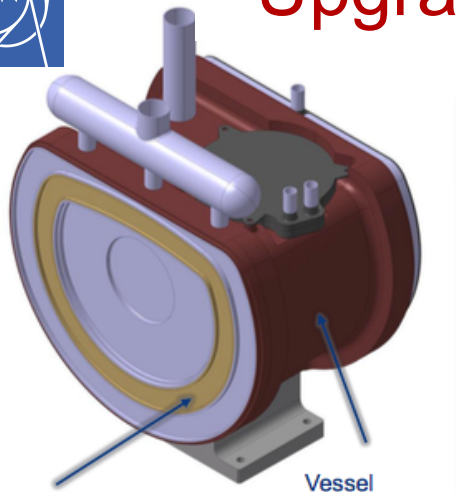

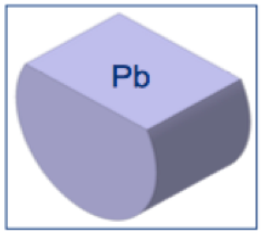

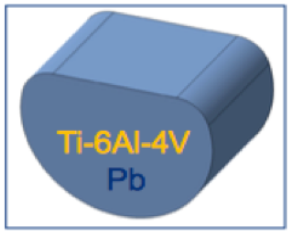

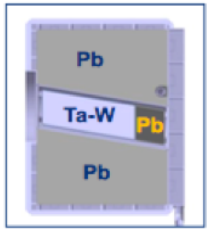

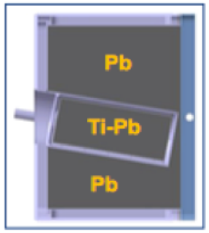

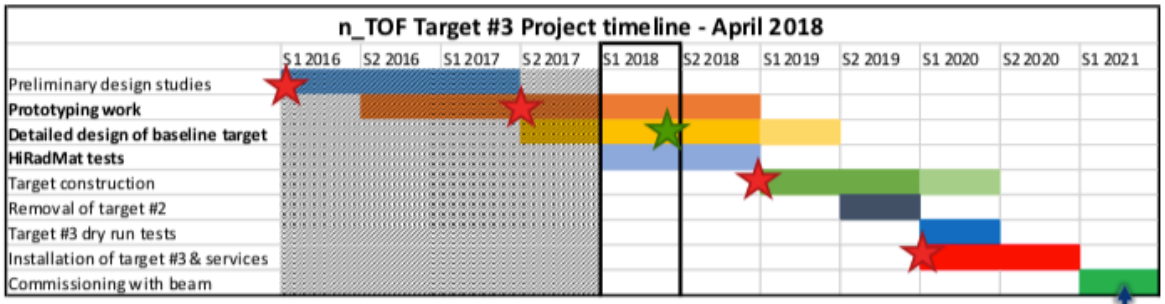

More flux

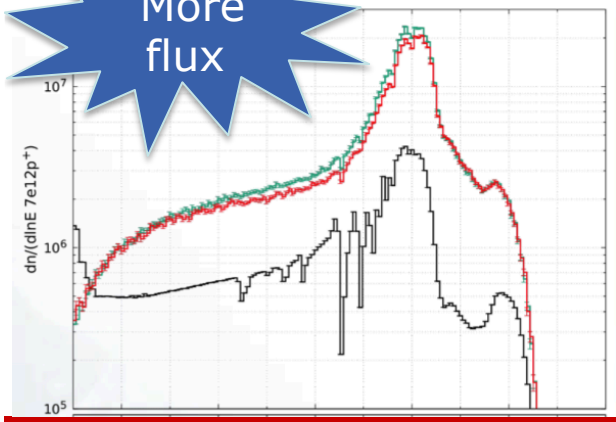

- T3 Project started early 2016
- Preliminary Design Review (PDR) June 2017 (EDMS 1837722)
- Intermediate Engineering Design Review (IEDR) 15th May 2018 (link)
- Production Readiness Review (PRR) Q4 2018
- Target Installation Review (TIR) Q1 2020
- *Target installation foreseen Q2 2020 + Beam on target S1 2021*

Future 2021 - 2030

Upgrade: new detector concept

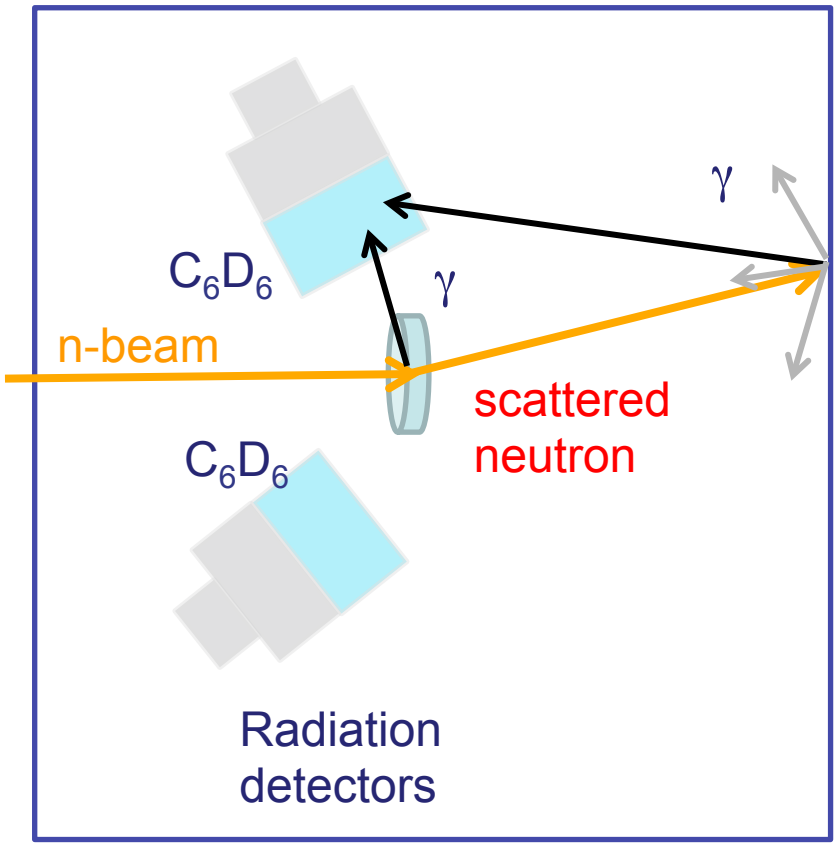

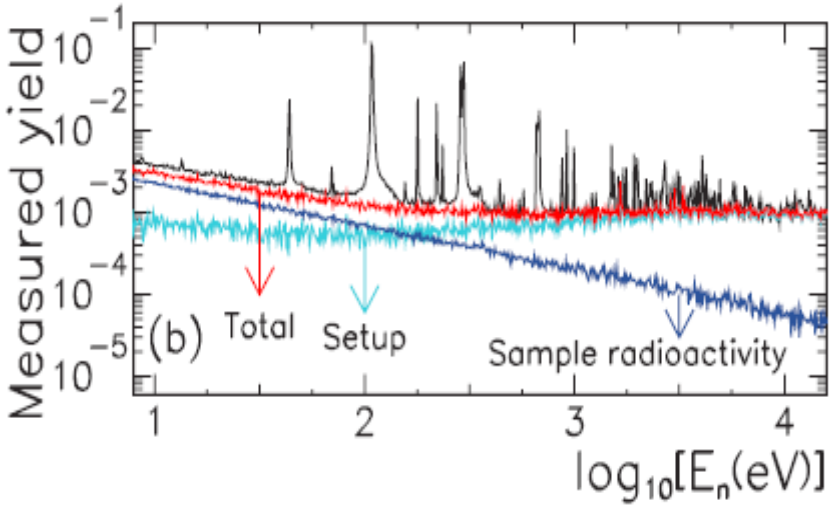

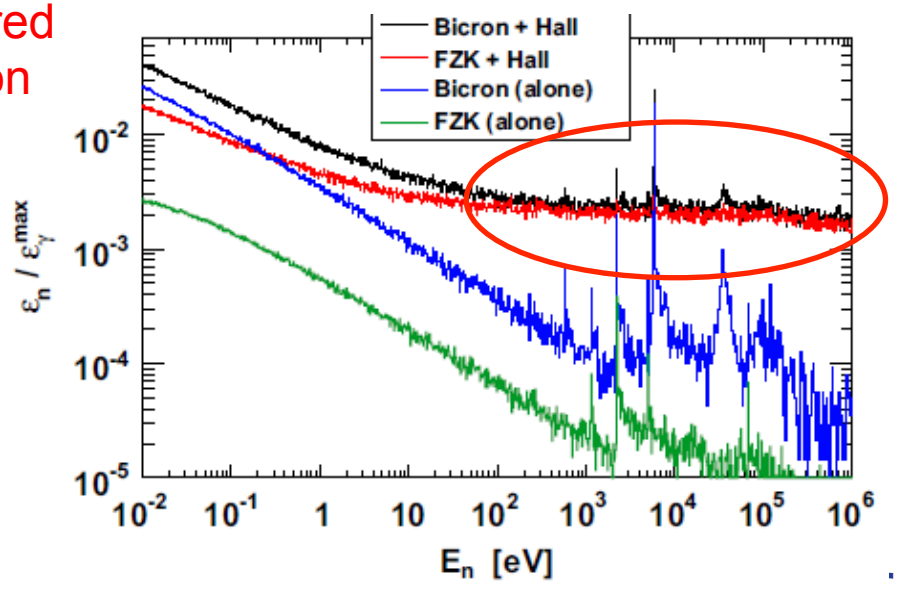

Future 2021 - 2030

Upgrade: new detector concept

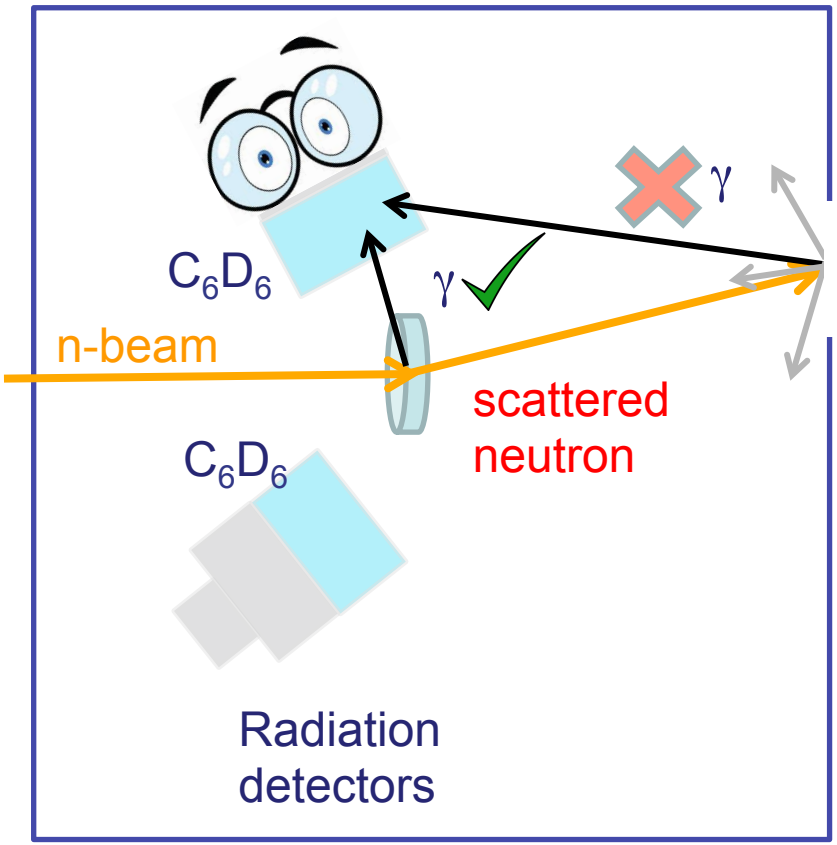

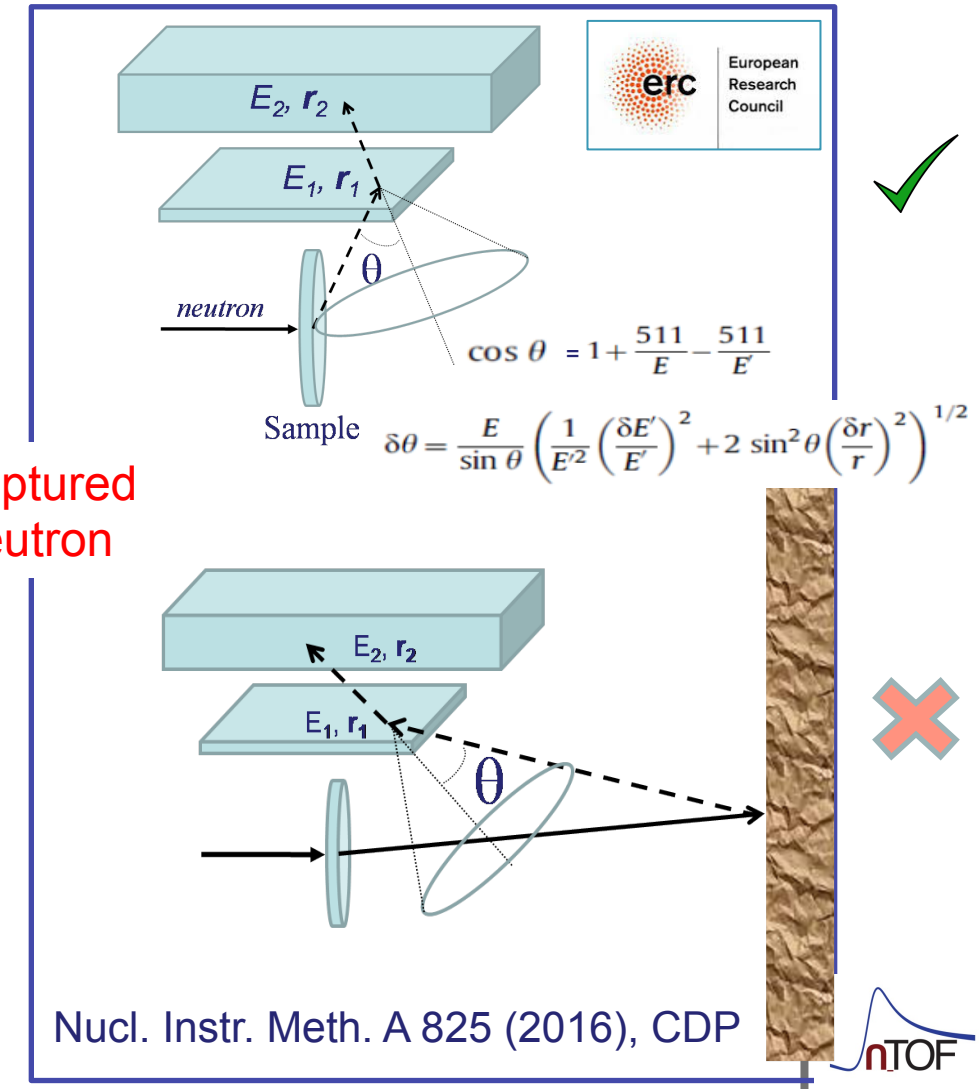

Conclusions

The n_TOF effort to improve cross section data for s process

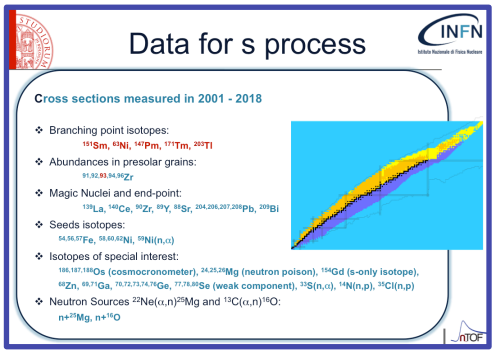

Conclusions

The n_TOF effort to improve cross section data for s process

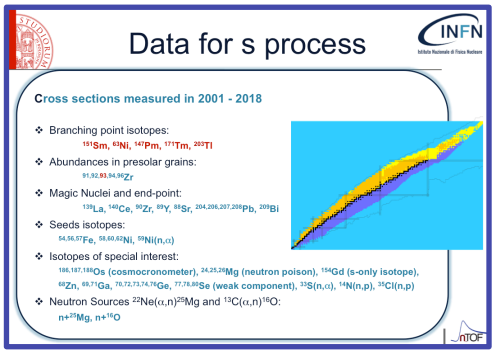

In the future (~ 2021 – 2030) challenging measurements: upgrade of the n_TOF facility and instrumentations

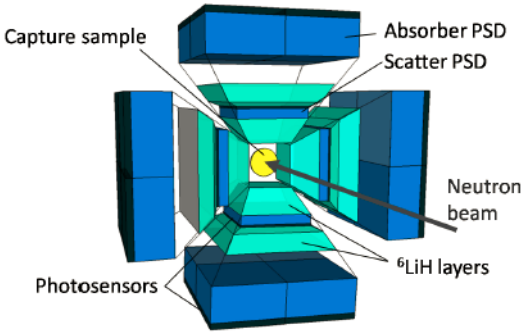

Conclusions

The n_TOF effort to improve cross section data for s process

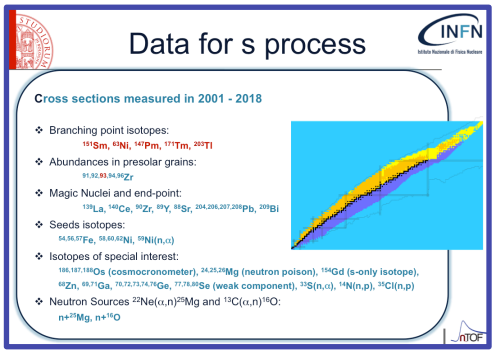

In the future (~ 2021 – 2030) challenging measurements: upgrade of the n_TOF facility and instrumentations

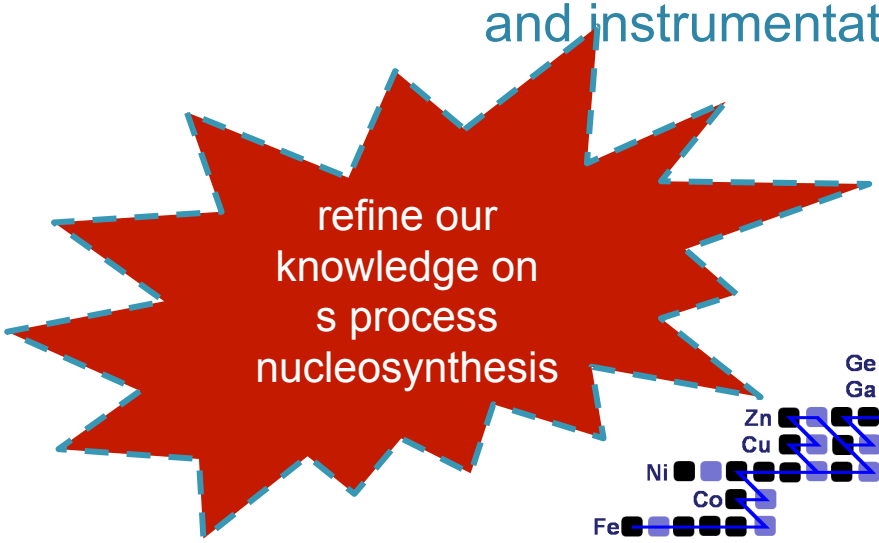

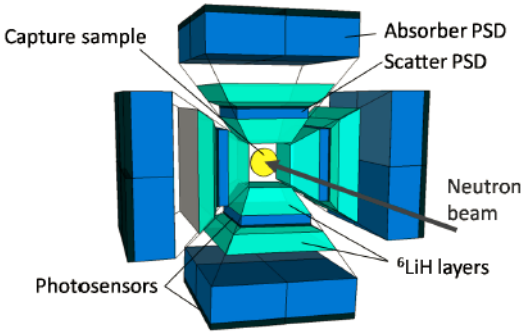

Conclusions

s process

"Easy" to be reproduced with an exponential distribution of neutron exposures.

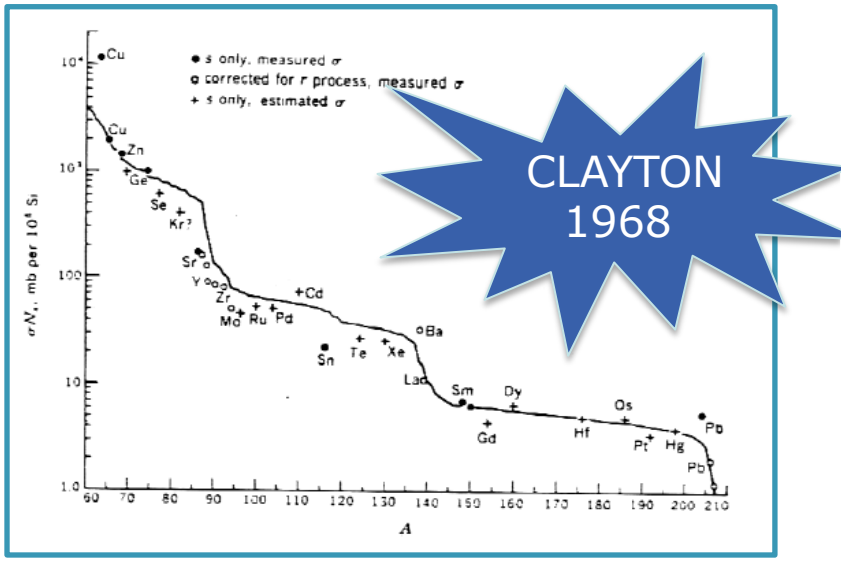

Moreover, given that the *s*-process occurs in a relatively low neutron-density environment, the neutron flow reaches equilibrium between nuclei with magic neutron numbers, where the product of the Maxwellian averaged stellar (n,γ) cross section of a nuclide, $\langle\sigma\rangle$, and its corresponding abundance, N_s, remains almost constant (the difference in the two product is much smaller than the magnitude of either one of them):

$$\langle\sigma\rangle_A N_A \approx \langle\sigma\rangle_{A+1} N_{A+1}$$

LOCAL APPROXIMATION

Conclusions

r process

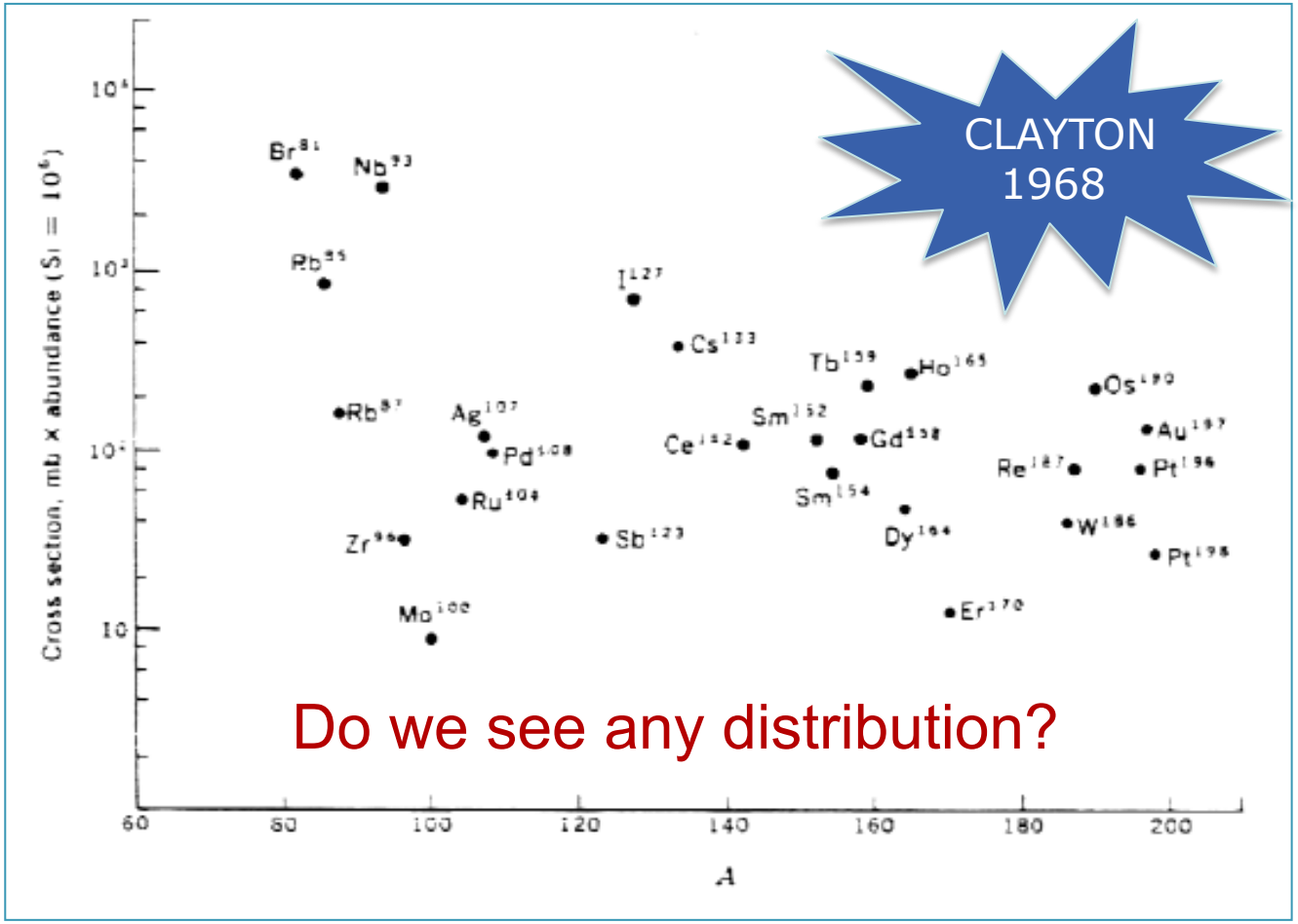

ALMA MATER STUDIORUM
UNIVERSITÀ DI BOLOGNA

Cristian Massimi
Dipartimento di Fisica e Astronomia
massimi@bo.infn.it

www.unibo.it